C. W. Bauschlicher, Jr. P. S. Bagus H. F. Schaefer III

Model Study in Chemisorption: Molecular Orbital Cluster Theory for Atomic Hydrogen on Be(0001)

Abstract: The interaction between atomic hydrogen and the (0001) surface of Be has been studied by using clusters of Be atoms to simulate the substrate. The largest cluster used contains 22 Be atoms, 14 in the first layer and 8 in a second layer. An H atom is added to the Be clusters at four high symmetry adsorption sites. Ab initio molecular orbital Hartree-Fock wave functions have been obtained and the interaction energy of H with the Be cluster is studied as a function of vertical distance from the surface. Thorough studies of various aspects of the computations and of the appropriate interpretation of the cluster results are reported. Our results show that three of the sites considered have similar binding energies, $D_e \approx 50 \text{ kcal/mol}$ ($\approx 2.1 \times 10^5 \text{ J/mol}$), and (vertical) equilibrium distances from the surface, $r_e \approx 0.1 \text{ nm}$. For the fourth site, H directly over a Be atom, $D_e \text{ is } \approx 30 \text{ kcal/mol}$ ($1.3 \times 10^5 \text{ J/mol}$), and $r_e \text{ is } \approx 0.14 \text{ nm}$. We expect that the dissociative adsorption of H_2 on Be(0001) will be exothermic. A model calculation for diffusion of H into the bulk indicates that this process is energetically unfavorable for an ideal (0001) surface. The vibrational energies for the motion of H normal to the surface are found to be substantially different for sites with different surface coordinations. The nature of the covalent bond formed between H and Be(0001) is analyzed.

1. Introduction

There has been a great deal of interest in the problem of chemisorption [1]. The binding energies of various adsorbed atoms and molecules are known for a variety of materials and there exists a wealth of other data obtained by photoelectron spectroscopy (ESCA or XPS), low energy electron diffraction (LEED), and other spectroscopies. Much has been learned from these experiments but there are some questions that are not easily answered. Among them are, for example, the nature of the bonding, site preference, the mechanisms of dissociative adsorption, and the changes in charge distributions upon adsorption. Ab initio molecular orbital theory has shown itself capable of answering these types of questions for many small molecules [2]. Application of the same techniques to the surfaces of solids could add to the understanding of chemisorption and aid in the interpretation of experimen-

Within the past five years, many molecular orbital calculations relating to surface electronic structure and chemisorption and involving small clusters of metal atoms have been performed. By far the largest number of these calculations [3–16] have used semi-empirical methods or the local, $\rho^{1/3}$, approximation for exchange. It is clear that many systems of interest are difficult to treat

with current *ab initio* techniques; other methods must be used. One use of this work and other *ab initio* [17-24] calculations is in helping to calibrate and evaluate semi-empirical methods for surface calculations.

With an ab initio molecular orbital approach, we are likely to be restricted to clusters of about 30 metal atoms, even with light atoms such as Be or Li. Although a cluster of 30 atoms may not yet have metallic properties, it may still be possible to study chemisorption. We are not interested in the bulk properties of the metal, but rather in what occurs at the surface during chemisorption. It is reasonable to consider that the bonding of an adatom to a surface is strongly dominated by the interaction of the adatom with its near neighbors on the surface; i.e., that the bonding is local in nature. In this case the cluster need only be large enough so that the atoms directly involved in the bonding do not feel large "edge effects" due to the finite size of the cluster. If this can be achieved, a molecular orbital approach to chemisorption would be desirable because it has the ability to accurately describe the local bonding.

In this paper, we consider the chemisorption of H on the (0001) surface of Be. We have obtained self-consistent field (SCF) wave functions for clusters of n Be atoms

Copyright 1978 by International Business Machines Corporation. Copying is permitted without payment of royalty provided that (1) each reproduction is done without alteration and (2) the *Journal* reference and IBM copyright notice are included on the first page. The title and abstract may be used without further permission in computer-based and other information-service systems. Permission to *republish* other excerpts should be obtained from the Editor.

Table 1 Experimental and calculated values of the dissociation energy $D_{\rm e}$ and the equilibrium bond length $r_{\rm e}$ for BeH. The calculations involve different basis sets and theoretical methods. For the SCF calculations, $D_{\rm e}$ is defined as the difference between the SCF energy of the molecule at $r_{\rm e}$ and the SCF energies of the separated atoms Be($^{\rm I}$ S) and H($^{\rm 2}$ S). The basis sets used in the present work are described in Section 3.

Method	$r_{\rm e}({\rm nm})$	D _e [kcal/mol; J/mol (10 ⁵)]
SCF (present work)		
Minimum Basis I	0.1420	46.4; 1.94
Double Zeta Basis I	0.1352	44.5; 1.86
SCF (large basis)[26] Near Hartree-Fock limit	0.1338	50.3; 2.11
Large configuration interaction [26]	0.1345	$48.8 \pm 0.7; 2.04 \pm 0.03$
Experiment [27]	0.1343	49.8 ± 0.2; 2.09 ± 0.008

 (Be_n) chosen to model the (0001) surface. The number of atoms ranges from 1 to 22. To the Be_n clusters we have added an H atom (Be_n-H) . The H atom has been placed in four adsorption sites and the vertical distance from the Be_n cluster has been varied. We have also obtained SCF wave functions for these Be_n-H systems. Several chemisorption properties, including bond energies, equilibrium geometries, and surface force constants, have been determined by using the Be_n and Be_n-H wave functions.

For the smaller clusters, we have been able to use both minimum and extended (double zeta) Gaussian basis sets [2] for the SCF calculations. For the larger clusters, only minimum basis sets could be used. Tests for the smaller clusters showed that the minimum basis set SCF wave functions gave reasonable results. Results for the larger clusters showed that the chemisorption properties were reasonably well converged with respect to cluster size.

There are several reasons for choosing a beryllium substrate. 1) Since the Be atom has four electrons, only relatively small basis sets are required; Li is the other small metal. This fact allows us to treat large clusters. 2) Be has a closed-shell ¹S ground state and the metal is known to have no magnetic properties [25]. Thus, the larger clusters would be expected to have closed-shell singlet ground states. This simplifies our theoretical treatment since we do not have to investigate configurations with several open shells. 3) The SCF approximation is reasonably accurate for BeH, the simplest Be,-H system. In Table 1, we give a comparison for several calculations of the dissociation energy D_{μ} and the equilibrium bond distance r_{e} for BeH. We note, in particular, that the minimum basis set SCF results (where the Be basis set includes a single 2p function) are in reasonable agreement with accurate theoretical configuration-interaction (CI)

[26] and experimental values [27]. 4) The bonding in BeH is essentially covalent and involves substantial 2p hybridization of the Be 2s orbital [26]. A minimum basis set (optimized for the neutral atoms) can be used to describe the bonding and interaction energies in this case. A minimum basis set would not be expected to be satisfactory for a case where the bonding had substantial ionic character, e.g., as might be expected for oxygen adsorption. For small Be,-H clusters [21, 24] the bonding of H remains covalent and a minimum basis set can also describe the cluster D_a and r_a fairly well. On the basis of considerations of the relative positions of energy levels, Schrieffer [28] has argued that an adsorbed atom will be neutral (covalently bonded) if its ionization potential IP is greater than the substrate work function ϕ , and if its electron affinity EA is less than ϕ . This is clearly satisfied for H on Be since for H, IP = 13.6 eV and EA = 0.75 eV [29], and for Be, $\phi = 3.8 \text{ eV}$ [30]. From all these considerations, we expect that a minimum basis set can be used for the larger clusters where calculations with a double zeta basis set would be very difficult.

There has not been a great deal of experimental work for chemisorption on beryllium, possibly because of the toxicity of Be metal. The interaction of H_2 , N_2 , O_2 , and CO with Be(0001) crystals and Be films has been studied [31]. It has been reported [31] that molecular hydrogen is not adsorbed on either surface. Low energy electron diffraction experiments [32] have shown that surface reconstruction does not occur for the (0001) surface. Finally, we note that Be surfaces have been studied by Auger electron spectroscopy [33].

Preliminary descriptions of the work presented in this paper, giving results for clusters of up to thirteen Be atoms, have already been presented [21, 24]. We now present results for larger clusters containing up to 22 Be atoms. We provide detailed information on the computational procedures and discuss, in particular, problems that arise from the application of molecular orbital theory to surface clusters. We also investigate the convergence of various properties of interest with respect to cluster size.

In Section 2, we describe the various clusters for which calculations have been performed and define a notation system to describe the clusters. The electronic states for which SCF calculations have been performed are also described. Section 3 deals with the computational details of the work. Extensive basis set tests are described. Other computational details related to convergence problems and methods used to determine the ground electronic states of the clusters are also discussed. In Section 4, the results of calculations on the Be_n clusters are reported. Several properties, e.g., ionization potential, cohesive energy, and singlet-triplet separation, are shown to measure edge effects in the cluster, rather than "bulk" prop-

erties of the metal. The results for the Be, -H clusters are given in Section 5. They are analyzed in terms of properties of the charge distributions. We discuss in detail the results for the chemisorption bond energies and bond distances for the various sites considered. The convergence of these properties with respect to cluster size is studied. In Section 6, we use the results given in previous sections to describe several features of the chemisorption of H on the Be(0001) surface. The relative stabilities of the four adsorption sites and the energetics of dissociative adsorption of H_a and of the diffusion of H into the crystal are all considered. The vibrational motion of the H atom normal to the Be surface is discussed, and the computed vibrational frequencies are analyzed in terms of a simple ball and spring model. The frequencies are shown to depend strongly on the coordination of the H adsorption site. In Section 7, the conclusions of this study are reviewed.

2. The cluster model

Since LEED studies [32] have shown that the (0001) surface of beryllium does not reconstruct, we use the structure of the bulk metal in all our cluster calculations. Beryllium has two atoms per unit cell and is described as being hexagonal close-packed [34], even though the c/a ratio (1.567) is somewhat smaller than the ideal value of $(8/3)^{1/2} = 1.633$. The (0001) surface is defined such that the surface normal is along the c axis [35]; each surface atom has nine near neighbors, six in the same layer and three in the layer below. The nearest-neighbor distance within a layer is 0.22866 nm, while the distance between the surface atoms and their neighbors below is shorter, being only 0.22255 nm [34]. Figure 1 shows the Be₉₉ cluster we used, illustrating the hexagonal close-packed structure of interest. This cluster, the largest considered, contains 14 atoms in the first layer, denoted 1 to 14, and 8 atoms in the second layer, denoted a to g. The cluster had C_e point group symmetry.

An H atom may be added to any one of four distinct high symmetry sites on the (0001) surface of Be. The sites and the specific choices of geometry for the Be₂₂-H cluster are as follows. 1) *Open site*—The H atom approaches the center of a triangle formed by three surface Be atoms (12, 13, and 14 in Fig. 1), where there is no second-layer Be atom below the H. 2) *Eclipsed site*—The H atom approaches the center of a triangle (11, 12, and 14), where there is a second-layer Be atom (g) below the H. 3) *Bond midpoint site*—The H atom approaches the center of a line joining two Be atoms (12 and 14). 4) *Directly overhead site*—The H atom approaches directly above one of the surface Be atoms (11). For all sites, the Be₂₀-H cluster has C₂ symmetry.

All of the clusters studied have one or two layers, and we have denoted this by enclosing the number of atoms in each layer in parentheses. For example, a six-atom clus-

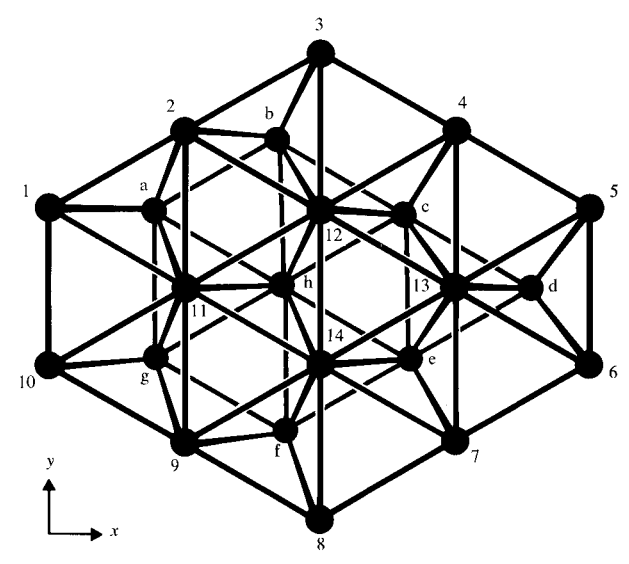


Figure 1 The $Be_{22}(14,8)$ cluster. This cluster illustrates the (0001) surface used in our studies of hydrogen adsorption on beryllium. The atoms in the first layer are denoted by numbers, those in the second layer by letters.

ter with all the atoms in the first layer is denoted $Be_6(6,0)$. The Be_{22} cluster in Fig. 1 is denoted $Be_{22}(14,8)$. For clusters other than $Be_{22}(14,8)$, the geometries and adsorption sites used are described in Appendix A.

All the results reported in this paper are based on single configuration SCF wave functions. Since Be metal is nonmagnetic [25], we would expect that the ground state of a cluster that simulates condensed Be would be a closedshell singlet. In some cases, edge effects for the finite clusters have led to a double-open-shell configuration which has a lower energy than the lowest closed-shell configuration. However, we shall refer to the lowest SCF closed-shell state of Be, as its "ground state." We have obtained SCF wave functions for this ground state and for the lowest triplet coupled double-open-shell states of the various Be, clusters. We have also determined the first ionization potential for Be, by obtaining the lowest singleopen-shell (doublet) configuration SCF wave function for the ion. For the Be,-H clusters, we have obtained SCF wave functions for the lowest single-open-shell doublet state. For each site considered on any Be, cluster, we have varied the vertical distance of the H atom from the top layer of the cluster in order to obtain a minimum of the SCF energy of Be_n-H. We call the vertical distance for which the energy is minimum the equilibrium bond length r_e. The binding energy of H to form Be_n-H (chemisorption bond energy) is obtained as the difference between the Be_n -H SCF energy at r_e and the SCF energies of Be_n (closed-shell ground state) and of H(2S).

Table 2 Equilibrium bond lengths $r_{\rm e}$ and binding energies $D_{\rm e}$ obtained with different basis sets for Be₇(7,0)-H and Be₁₀(10,0)-H clusters. Descriptions of the clusters and adsorption sites are given in Section 2 and Appendix A.

Cluster and site	Basis set	r _e (nm)	$D_{\rm e}$ [kcal/mol; J/mol (10 5)]
$Be_{7}(7,0),$	Minimum I	0.143	71.3; 2.99
directly	Minimum IIb	0.139	73.9; 3.10
overhead	Double Zeta I	0.139	60.9; 2.55
	Double Zeta II	0.138	64.0; 2.68
$Be_{10}(10,0),$	Minimum I	0.116	31.5; 1.33
bond	Minimum III	0.111	32.9; 1.38
midpoint	Double Zeta I	0.110	38.4; 1.61
	Double Zeta II	0.106	35.8; 1.50

Table 3 Equilibrium bond lengths r_e and binding energies D_e obtained with different basis sets for Be_n-H, n = 3 to 7 clusters.

Cluster and site	Basis set	r _e (nm)	$D_{\rm e}$ [kcal/mol; J/mol (10 ⁵)]
Be ₃ (3,0), open	Minimum I	0.125	19.1; 0.80
	Minimum IIb	0.117	22.5; 0.94
	Double Zeta I	0.110	22.0; 0.92
Be ₄ (3,1), eclipsed	Minimum I	0.124	28.7; 1.20
	Double Zeta I	0.117	33.0; 1.38
Be ₄ (4,0), bond midpoint	Minimum I Double Zeta I	0.126 0.119	70.1; 2.94 65.4; 2.74
Be ₅ (4,1), open	Minimum I	0.102	23.2; 0.97
	Double Zeta I	0.091	31.9; 1.35
Be ₅ (4,1), eclipsed	Minimum I	0.115	30.1; 1.26
	Double Zeta I	0.106	36.4; 1.53
Be ₅ (4,1), bond midpoint	Minimum I Double Zeta I	0.114 0.106	32.4; 1.36 38.1; 1.60
$Be_6(6,0),$ open	Minimum I	0.118	47.3; 1.98
	Double Zeta II	0.106	45.9; 1.92
Be ₆ $(3,3)$, open	Minimum I	0.111	55.3; 2.32
	Double Zeta II	0.103	60.6; 2.54
Be ₇ (6,1), eclipsed	Minimum I	0.111	40.8; 1.71
	Double Zeta II	0.102	47.8; 2.00

3. Computational details

A. Basis set tests

In any ab initio calculation, the choice of the basis set [36] is extremely important and determines whether the wave function will give an accurate description of the system of interest. Special care must be taken when a minimum basis set is used. Several different basis sets of contracted Gaussian functions were tested, the primary objectives being to obtain a minimum basis set suitable for use with

larger clusters, and to determine the quality of this set for the calculation of chemisorption properties. We believe that the tests support the reliability of the minimum basis set used in the larger clusters.

The minimum basis sets consisted of three contracted Gaussian functions centered on each Be atom, denoted 1s, 2s, and 2p, and a 1s function centered on H. (All three components of the 2p function are included in the basis set.) Four basis sets of this type were used. In Minimum Basis Set I, the Be parameters are those optimized for the free atom. In Minimum Basis Sets IIa and IIb, the Be 2s and 2p parameters were optimized for use in the Be₁₃(10,3)A cluster [see Appendix Fig. A1(f)]. For Set IIa, the Gaussian functions used to represent the 2s and 2p basis functions were constrained to have the same exponents, while for Set IIb, this constraint was not imposed. In Minimum Basis Set III, the 2s and 2p parameters were optimized for use in the Be₁₀(10,0) cluster. Sets Ilb and III are very similar to each other. The double zeta basis sets contain two functions of each type (1s, 1s', 2s, 2s', etc.) on each atom. In addition, a single p function on H was used. Roos and Siegbahn [37] have discussed the importance of including this function in double zeta basis sets. Two sets, Double Zeta I and II, were studied. They differ only in the Gaussian functions used to form the two Be 2p basis functions. Set II uses four elementary Gaussian functions for this purpose rather than the two used in Set I. This allows a better description of the Be 2p character, which was found to be quite important for bonding in the clusters. Details concerning the basis sets and tables of the parameters used are given in Appendix

The evaluation of the basis sets was based on comparison among the calculated values (using different basis sets) for the equilibrium bond distance and the binding energy of adsorbed H. For several small clusters, these values are tabulated in Tables 2 and 3. (Except for the Be(10,0) cluster, no spatial symmetry constraints [2, 38] were imposed on the SCF wave functions used for the tables. For Be₁₀(10,0), the molecular orbitals were of D_{2h} symmetry for Be₁₀ and of C_{2v} symmetry for Be₁₀-H. In all cases, spin symmetry was imposed; the α and β spin orbitals for a given shell have the same spatial dependence.)

Calculations for the smaller clusters were performed by using Minimum Basis Set I. These calculations showed that p functions were very important for several clusters, as seen for the ground state configuration of Be₇(7,0). The D_{6h}-symmetry ground state occupation expected from seven Be atoms with configuration $1s^22s^2$ is (1s cores) $3a_{1g}^22e_{1u}^42e_{2g}^42b_{1g}^24a_{1g}^2[39]$, where the molecular orbitals (MO) are ordered according to the expected SCF orbital energy ε ; ε (3a_{1g}) < ε (2e_{1u}), etc. However, the SCF ground state was actually found to be (1s cores) $3a_{1g}^22e_{1u}^42e_{2g}^41b_{2u}^24a_{1g}^2$. The $1b_{2u}$ MO can be formed only from combinations

of Be p basis functions. It is possible that Minimum Basis Set I might be favoring the p functions in such a way as to predict the wrong ground state. The SCF wave function for the cluster was recomputed by using both double zeta basis sets; the ground state configuration was found to be the same. The same problem was noted for the $Be_{10}(10,0)$ cluster. Here also, the double zeta basis sets gave the same ground state configuration as the minimum basis set. We conclude that the importance of the p functions is not a basis set artifact.

A measure of the importance of the Be 2p character may be obtained from a Mulliken gross population analysis [2]. For Be₁₀(10,0), the 2p character per atom ranges from 1.1 to 1.5 electrons [21]. Clearly, the charge distribution around a Be atom in a cluster is very different from the 1s²2s² free atom. For this reason, we optimized the parameters of the minimum basis set Be 2s and 2p functions for the Be₁₀(10,0) cluster. The resulting basis set is denoted Minimum Basis Set III. With this basis set, the cohesive energy (binding energy per atom) of Be₁₀(10,0) increased from 8.9 kcal/mol (3.73 × 10⁴ J/mol) (Minimum Basis Set I) to 12.2 kcal/mol (5.11 \times 10⁴ J/mol). However, as shown in Table 2, the changes in the bond energy and distance for H chemisorption were small. The Be 2s and 2p parameters were also optimized for the Be₁₀(10,3)A cluster to obtain Minimum Basis Sets IIa and IIb. With these basis sets, the cohesive energies of the $Be_{\alpha}(7,0)$ [Set IIb] and Be₁₂(10,3)A [Set IIa] clusters increased by 3 kcal/ mol $(1.3 \times 10^4 \text{ J/mol})$ over the Minimum Basis Set I values. However, for $Be_7(7,0)$, as for Be_{10} , the effect on the chemisorption properties was small (cf. Table 2). Although the use of the optimized minimum basis sets increased the cohesive energies of the clusters by approximately 30 percent, only small changes occurred in the chemisorption properties. The bond lengths for $Be_{\pi}(7,0)$ and Be₁₀(10,0) shorten and lie between the Minimum Basis I and the double zeta basis set results. The bond energies change by less than five percent. In general, the minimum basis description of chemisorption is very reasonable. The bond energies are within 20 percent of the double zeta results, except for the Be₋(4,1) open site, where the Minimum Basis I yields only 75 percent of the Double Zeta I value. They are usually smaller than the double zeta values, although Be₂(7,0) and Be₄(4,0) are exceptions to this. These clusters have large edge effects that cause anomalous binding energies. For all of the larger clusters, the minimum basis binding energy is, therefore, expected to be too small. The minimum basis set bond lengths are all ≈0.01 nm longer than the double zeta values.

B. Selection of the ground state electronic configuration The description of the electronic configuration (i.e., numbers of singly and doubly occupied MOs in each symmetry) is an item of input for an SCF calculation. If the input configuration is not that of the ground state, the SCF procedure will naturally converge to an excited state. For most molecules, chemical intuition and group theoretic analysis lead to a correct determination of the ground state configuration. For clusters of Be atoms designed to model surface and bulk properties, the determination of the ground state configuration is not a trivial matter.

In order to determine the ground state configuration, we obtained the 4n electron SCF wave function for the larger clusters in several steps. First, we obtained a 2n electron wave function with only the $n ext{ 1s}^2 ext{ MOs occupied}$. Then we added 2m electrons in the lowest m (unoccupied) virtual orbitals of the previous SCF wave function and iterated to self-consistency. This step was repeated until all the electrons were included. This procedure of adding electrons a few at a time to the virtual orbitals with the lowest eigenvalues was particularly useful for choosing, among orbitals of the same symmetry, which to occupy and which to leave unoccupied. It was, however, not foolproof for choosing between orbitals of different symmetry having the same orbital energy [within about 0.05 hartree (1 hartree = 2 rydbergs = 27.212 eV)]. This was important only in the final steps of the procedure when almost 4n electrons were included in the wave function. When it occurred, both possible occupations had to be tested with separate SCF calculations. In this way it was necessary to test only a small number of configurations in order to find the closed-shell ground state. Further, the configurations to be tested were clearly identified.

Even when the ground state configuration is correct as to the number of occupied orbitals in each symmetry, it is still possible to converge to an excited state. This is easily seen for the Be atom. If we require only that the ground state have two doubly occupied s shells, it is possible to converge to the highly excited state 1s²3s². For the Be atom, it is trivial to avoid this problem, but for larger Be clusters, differences among the orbital energies of the highest occupied MOs become fairly small. For Be₂₂, the average difference between the energies of adjacent MOs for the highest five occupied levels is only 0.23 eV. When the MOs show this "bandlike" behavior, it is difficult to be sure that the SCF process has not converged to an excited state. It might be possible to converge to a state where a level somewhat above the Fermi level is filled and one somewhat below is empty. It is not useful to try to detect such an excited state by comparing the orbital energies of the occupied and virtual MOs of the final, 4n electron wave function. In the Hartree-Fock method [40], the energies of the canonical virtual orbitals are defined differently from those of the occupied orbitals. Our procedure of adding electrons in steps should allow us to avoid these excited states. In this procedure, we choose which orbitals to occupy only from among the virtuals. The or-

C _{3v} MO basis	C _s MO expansion coefficients				
	3a'	4a'	5a'	2a"	
Occupied					
la,	-0.0001	+0.0001	-0.0001	_	
$2a_1$	+0.9984	+0.0050	+0.0551	_	
$3a_1$	+0.0153	+0.9236	-0.3721	_	
1e	-0.0002	+0.0004	-0.0001	+0.0008	
2e	-0.0487	+0.3825	+0.8831	+0.9996	
Virtual					
4a ₁	-0.0133	+0.0181	+0.1852	_	
5a ₁	+0.0006	-0.0104	-0.0214		
3e	-0.0168	+0.0090	+0.1986	+0.0183	
4e	+0.0069	-0.0040	-0.0666	+0.0112	
5e	+0.0049	-0.0063	+0.0051	+0.0132	
$1a_2$			_	+0.014	

bital energies of the virtual MOs are all defined in the same way and it is reasonable to choose to occupy a virtual MO with a lower energy and leave one with a higher energy unoccupied. With these orbitals as a starting point, we expect the SCF iterations to converge to the lowest state of the given configuration.

However, for Be₁₄(14,0) and Be₂₂(14,8) we did make a final check to ensure that we had indeed obtained the ground state wave function. We formed a set of configurations by removing one electron from an occupied MO (ϕ_0) and placing it in a virtual MO (ϕ_v) . (For Be₁₄, we removed the electron from one of the ten occupied MOs with the highest orbital energies and placed it in one of ten low-lying virtual MOs. For Be,, the electron was removed from one of the 22 highest occupied MOs and placed in one of 25 virtuals.) The configurations were linear combinations of two determinants so that the total wave function was a singlet. Only one of these configurations had an energy less than 1 eV above that of the closed-shell SCF wave function. In this one case (for Be₁₄), the energy was 0.07 eV above the closed-shell state. We formed a new closed-shell state by placing both electrons in the appropriate ϕ_v , leaving ϕ_o unoccupied. Starting with these orbitals, a new SCF wave function was obtained and its energy was higher than that previously obtained. Since all other configurations had considerably higher energies, we assumed that none of them would lead to a new closed-shell ground state.

For Be_n^+ and the triplet states of Be_n , much simpler procedures were followed. For Be_n^+ , we simply removed an electron from the occupied orbital with the highest orbital energy and used the ground state MOs as a starting point for the SCF iterations. For the triplet state, the electron was removed from the highest occupied orbital and

placed in the lowest virtual orbital, and the SCF calculation was performed. No tests were made to determine whether these configurations were the lowest states.

For Be,-H, we added an electron in a singly occupied orbital to the closed-shell Be, ground state. As we show in the next section, this procedure can easily lead to excited state configurations when the Be -H cluster has a point group symmetry higher than C_s. For this reason, we report results for SCF wave functions obtained by using either no spatial symmetry at all or C_a symmetry, even though the Be, -H cluster may have had higher symmetry. When C_s symmetry was used, the open-shell orbital was placed in both a' and a" symmetries and the configuration with the lowest SCF energy was taken as the ground state. The initial guess of the MOs for Be,-H, at the first hydrogen-to-cluster distance for which an SCF calculation was performed, consisted of the doubly-occupied Be, orbitals plus a singly-occupied 1s orbital on hydrogen. Even though the self-consistent MOs are quite different from these trial functions (see Section 5), the density matrix derived from them corresponds to a neutral H and a neutral Be, cluster, and is sufficiently good that the calculations converged. At other hydrogen distances, the trial functions were chosen as the converged MOs at a nearby distance for the same cluster and site.

C. Symmetry considerations; ground state configuration of Be_-H

One of the most puzzling aspects of our earlier work [21, 24] was a large change in the chemisorptive bond energy when we changed from a spatially-restricted to a spatially-unrestricted wave function [2, 38]. One cluster showing this effect was $Be_3(3,0)$, which has D_{3h} symmetry [see Appendix A, Fig. A1(a)]. The H atom is added to the open site and $Be_3(3,0)$ -H has C_{3v} symmetry.

We performed two sets of SCF calculations for Be₃ and Be₃-H. In the first set, we constrained the MOs to have the symmetry of the point group of the cluster: D_{3h} for Be₃ and C_{3v} for Be₃-H. In the second set, we only constrained the MOs to have C_s symmetry. The C_s reflection plane used was one of the three equivalent σ_v planes of D_{3h} or C_{3v} .

The ground state configuration of the Be₃ cluster was found to be

$$1a_1^{'2}1e^{'4}2a_1^{'2}2e^{'4},$$
 (1)

where $1a_1'$ and 1e' are the 1s cores of Be. We obtained this fully symmetry-adopted result even when we imposed only the C_s constraint [38, 41]. The hydrogen 1s orbital transforms as $a_1(C_{3v}$ symmetry). Hence, we assumed that the ground state configuration of Be₃-H would be

$$1a_1^2 1e^4 2a_1^2 2e^4 3a_1(^2 A_1). (2)$$

Table 5 Equilibrium bond lengths r_e , binding energies D_e , and total energies E_{tot} , at r_e for Be₃-H obtained with different wave functions and for different states.

Type of calculation and state	$r_{\rm e}({\rm nm})$	$D_{\rm e}$ [kcal/mol; J/mol (104)]	E_{tot} (eV; hartrees)
SCF, ² A ₁ , C _{3v} ; Eq. (2)	0.102	6.16; 2.58	-1187.7; -43.64793
CI, ² A ₁ , C _{3v}	0.106	17.72; 7.42	-1191.2; -43.77335
SCF, ² E, C _{3v} ; Eq. (4)	0.121	19.23; 8.06	-1188.3; -43.66876
SCF, 2A', Cs; Eq. (3)	0.117	22.48; 9.42	-1188.5; -43.67394
CI, ² E, C _{3v}	0.122	23.59; 9.88	-1191.4; -43.78270

The correspondence between C_{3v} and C_s symmetry is such that the a' representation of C_s contains the a_1 and one component of the e representation of C_{3v} . The a" representation of C_s contains a_2 and the other component of e. Thus, in C_s Eq. (2) becomes

$$3a'^24a'^22a''^25a'(^2A'),$$
 (3)

where only the valence shells are shown. With the C_{3v} symmetry constraint (and by using Minimum Basis Set IIb), the SCF results were obtained for the 2A_1 state of Eq. (2). The binding energy of H was 6.2 kcal/mol (2.60 \times 10^4 J/mol) and the equilibrium bond length (distance of H from the Be $_3$ plane) was 0.102 nm. When the calculations were performed with only the C_s symmetry constraint [Eq. (3)], the results were very different. The binding energy increased by a factor of three [to 22.5 kcal/mol (9.43 \times 10^4 J/mol)] and the bond length increased by 0.015 nm (to 0.117 nm).

In order to interpret the large differences between the C_s and C_{av} results, we performed C_s SCF calculations on Be_3 -H, using as basis functions the C_{3v} MOs (occupied and virtual) obtained from the C_{3v} SCF calculation on the ²A₁ state of Eq. (2). The results of the SCF calculations are, of course, identical whether the contracted Gaussian basis or the MO basis is used [42]. However, the character of the C_s MOs can be much more easily identified from the expansion coefficients when the C_{3v} MOs are used as the basis. For a representative H-to-Be distance (0.117 nm above the Be plane), these expansion coefficients are given in Table 4. If the C_s MOs had maintained the C_{3y} symmetry of Eq. (2), we would have had 3a' = $2a_1$, 4a' and 2a'' = 2e, and $5a' = 3a_1$. From Table 4, we see that the 3a' and 2a" MOs are very much what we expect them to be. The 4a' and 5a', however, are not at all as expected; the 4a' is dominantly 3a, and the 5a' is dominantly 2e. Thus, the C_{3v} configuration most closely resembling the C_s wave function is

$$2a_1^2 3a_1^2 2e^3(^2E)$$
. (4)

We then performed C_{3v} constrained SCF calculations for

this state. The hydrogen binding energy and bond length are, as shown in Table 5, quite close to the C_s results.

It is clear that the ²E configuration of Eq. (4) is the ground state of Be₂-H. It is also clear that most of the large apparent "symmetry-breaking" effects noted earlier are merely the result of our having assumed an incorrect ground state in C_{3v} symmetry. The use of the lower, C_s, constraint allowed the orbitals to reorganize so that the total wave function closely approximated the correct, ²E, ground state symmetry. The differences between the $C_{3v}^{2}E$ state results and the C_{s} results are the proper measure of the effect of removing the C_{3v} symmetry and equivalence restrictions [38]. These relatively small differences may be viewed as resulting from a partial inclusion of correlation effects in the C_s wave function. Large differences between the symmetry-constrained and unconstrained results [21, 24] are a good indication that the correct high symmetry ground state has not been found.

The closed-shell ground state SCF wave functions for Be_n were obtained by using both the appropriate high symmetry constraint and using either no symmetry or C_s symmetry. We always obtained the same total energy and electron density whether we imposed high symmetry or not [41]. For the triplet state of Be_n , for Be_n^+ , and for Be_n^- H, we report here only the results obtained by using no symmetry or C_s symmetry. We feel that these low symmetry results transform approximately as one of the representations of the appropriate high symmetry point group. However, except for Be_a -H, this was not checked.

Configuration-interaction (CI) calculations were performed for the $^2\mathrm{E}$ and $^2\mathrm{A}_1$ states of $\mathrm{Be}_3(3,0)\text{-H}$. Only excitations from the valence orbitals were allowed and the configurations were restricted to the interacting space [43]; that is, all singly- and doubly-excited configurations with a nonzero matrix element with either the configuration of Eq. (2), for $^2\mathrm{A}_1$, or Eq. (4), for $^2\mathrm{E}$, were included. The results of the CI computations are summarized in Table 5. The $^2\mathrm{E}$ state CI result is very similar to the C_s symmetry SCF result and suggests that our single configuration description is reasonably accurate. Unlike the $^2\mathrm{E}$, the $^2\mathrm{A}_1$ state has an extremely large correlation effect.

Table 6 Some properties of Be_n clusters. The results in parentheses were obtained by using the Double Zeta I Basis Set; all others were obtained by using a minimum basis, as described in Section 3D.

Cluster	ΔST (eV)	IP (eV)	$E_{\rm coh}$ [kcal/mol; J/mol (104)]
Be atom	1.78 (2.02)	8.44 (8.04)	
$Be_3(3,0)$	0.73(-0.98)	6.97 (6.47)	-5.03; $-2.11(-3.24$; -1.36)
$Be_4(3,1)$	1.15 (1.08)	7.18 (6.68)	4.07; 1.71(4.84; 2.03)
$Be_4(4,0)$	-1.18(-0.79)	5.13 (4.94)	-9.78; $-4.10(-6.69$; -2.80)
$Be_{s}(4,1)$	-0.68(-0.40)	5.73 (5.11)	0.23; 0.10(1.68; 0.70)
$Be_6(3,3)$	-0.43	5.30	1.81; 0.76
$Be_6(6,0)$	-0.24	5.58	-1.53; -0.64
$Be_7(6,1)$	-0.24	5.58	1.49; 0.62
$Be_7(7,0)$	-0.73	5.21	3.64; 1.53
$Be_{9}(6,3)$	-1.56	4.81	3.53; 1.48
$Be_{10}(7,3)$	0.04	6.05	8.98; 3.76
$Be_{10}(10,0)$	0.02	5.17	8.94; 3.75
$Be_{13}(10,3)A$	-0.62	4.32	14.15; 5.93
Be ₁₃ (10,3)B	-0.62	4.70	14.03; 5.88
Be ₁₄ (14,0)	-0.39	4.73	14.44; 6.05
Be ₂₂ (14,8)	not calculated	4.71	20.59; 8.63

D. Final choice of basis sets and wave function symmetry

For the results to be described below, the following choices were made unless otherwise noted. The clusters with ten or fewer Be atoms use Minimum Basis I. The two Be₁₃ clusters use Minimum Basis IIa and the Be₁₄ and Be₂₂ clusters use Minimum Basis IIb. (These basis sets are described in Section 3A and tabulated in Appendix B.) The SCF wave functions for clusters with ten or fewer Be atoms and Be₁₃(10,3)B [see Appendix A, Fig. A1(g)] were computed without any spatial symmetry restriction [38]. (The open-shell minimum basis set triplet state of Be₅(4,1) was computed in C_s symmetry to avoid convergence problems.) The wave functions involving the Be₁₃(10,3)A, Be₁₄, and Be₂₂ clusters were constrained to have C_s symmetry. All wave functions were spin restricted and are eigenfunctions of S^2 .

4. Results: clusters without H

The most serious questions about the use of cluster models are related to the fact that a finite and rather small number of atoms are used to model the surface of a crystal. The atoms at the edges or ends of the cluster are not in a proper long-range crystalline environment. We refer to the effects of these edge atoms on various properties of the cluster as "edge effects." Even for fairly large clusters, the number of edge atoms is large, especially when counted as the ratio of edge to interior atoms. (In the present context, we use "interior" to mean that an atom has the appropriate number of neighbors for a (0001) surface, not that it is in the interior of a model for the bulk crystal.) For our largest cluster, Be₂₂(14,8), only the four atoms in the first layer numbered 11 to 14 in Fig. 1 can be

clearly considered interior atoms. Atom h is in the interior of the second layer but lacks its nearest neighbors, which are in the third layer. At least 17 (77 percent) of the 22 Be atoms are clearly edge atoms. Our clusters were chosen to represent the (0001) surface. We could, with about the same number of atoms, have chosen configurations that would have had fewer atoms at edges or other nonequivalent positions, e.g., a linear chain. With such clusters, we would have been able to study edge effects in more detail, but clearly we could not have modeled the properties of the (0001) surface.

A second problem, closely related to that of edge effects, concerns the convergence of various properties as a function of cluster size. At first glance, it would seem that as the clusters become larger the computed properties would become less affected by the edge atoms. However, this is not always the case, as we shall show below; certain properties, e.g., the first ionization potential, are always likely to be strongly influenced by edge atoms.

In certain cases, it is possible to reduce or eliminate edge effects by including a model or effective crystalline environment into the cluster treatment. Cartling et al. [44] have done this for silicon. They terminated a five-atom cluster by saturating the dangling bonds of the edge Si atoms with hydrogens. For a covalently bonded semiconductor like Si, this is most likely to be a satisfactory procedure. However, for a metal like Be, where the conduction electrons are delocalized over the entire crystal, this approach is not suitable.

Edge effects may be important for both bare clusters and for clusters with H. However, the properties related to chemisorption involve differences between a cluster (Be_n) with an H atom at infinite distance and the Be_n-H

complex. Since we expect the adsorbate bonding to be local in character, it is likely that edge effects will be less important for the chemisorption properties. We now consider various properties of the bare clusters, emphasizing the characterization of the edge effects. (In the next section, we present a similar treatment of the properties of the Be₋-H clusters.)

Low-lying excited states of Be_n will be discussed first. As noted in Section 2, the ground states of the Be_n clusters are assumed to be closed-shell. If the clusters converge to metallic behavior, it is reasonable to expect that the energy separation between the closed-shell and the lowest double-open-shell state $(\varphi_{2n}^2 \to \varphi_{2n}^1 \varphi_{2n+1}^1)$ will go to zero as *n* becomes large (provided, of course, that these energies can be reasonably approximated by using Hartree-Fock wave functions). Further, if the orbitals φ_{2n} and φ_{2n+1} are delocalized over the cluster (Blochlike), the singlet and triplet coupled states arising from $\varphi_{2n}^1 \varphi_{2n+1}^1$ should have nearly the same energy as *n* becomes large.

We have computed SCF wave functions for the lowest open-shell triplet states of Be_n . The differences of the SCF energies of the lowest closed-shell state and this triplet state, denoted as the singlet-triplet separation ΔST ,

$$\Delta ST = E_{SCE}$$
(open-shell triplet) - E_{SCE} (closed shell), (5)

are given in Table 6. A negative value of ΔST indicates that the SCF energy of the triplet is lower than that of the closed shell. It can be noted from Table 6 that ΔST is negative for most of the clusters. For Be₁₃(10,3)A for example (see Appendix A, Fig. A1(f), the energy of the 16a'17a' 3 A' state is 0.6 eV lower than that of the lowest closed-shell 1 A', (16a') 2 state.

For the large clusters, the negative values of ΔST arise from edge effects coupled with limitations of MO SCF wave functions. This may be seen by considering the charge distributions (orbital densities) of the 16a' and 17a' orbitals of the ³A' state of Be₁₂(10,3)A, which are plotted in Figs. 2 and 3. (We emphasize that these orbitals are obtained from a SCF calculation on the triplet state; they are not taken from the ground state results.) Clearly, there are not bonding or antibonding orbitals distributed over the entire cluster. The orbitals are best described as being localized on the top and bottom of the cluster. A similar sort of behavior is seen for the H_a molecule at large internuclear separation [45], where the closed-shell MO SCF wave function, $1\sigma_g^2 = (1s_A + 1s_B)^2$, becomes very poor and has an energy considerably above that of the open-shell configuration 1s_A1s_B.

It is not possible from our calculations to separate the limitations of the closed-shell MO SCF wave function from the inherent edge effects. It is certainly possible that the lowest triplet state would involve excitations on edge atoms even if better wave functions were used. It is also possible that this would be true for finite clusters of arbi-

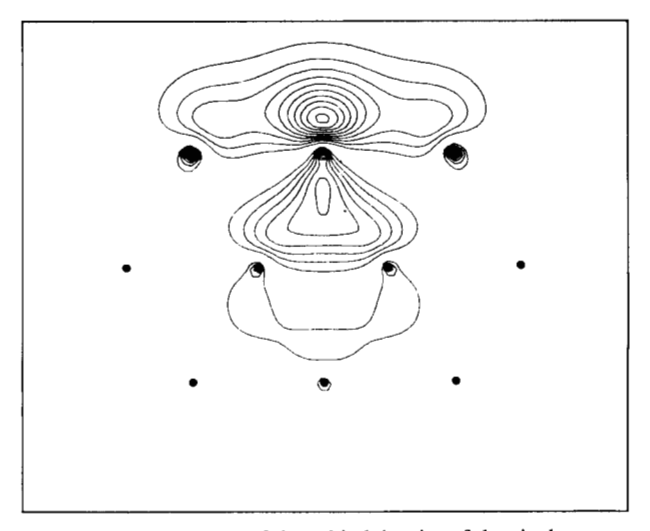


Figure 2 Contour plot of the orbital density of the singly-occupied 16a' SCF MO for the 3 A' state of the Be₁₃(10,3)A cluster. The plane of the plot is the top layer of the cluster; the positions of the Be atoms in this plane are marked [see also Appendix A, Fig. A1(f)]. The smallest contour value is 0.041 eV (1.5 × 10^{-3} hartree), as is the interval between contours.

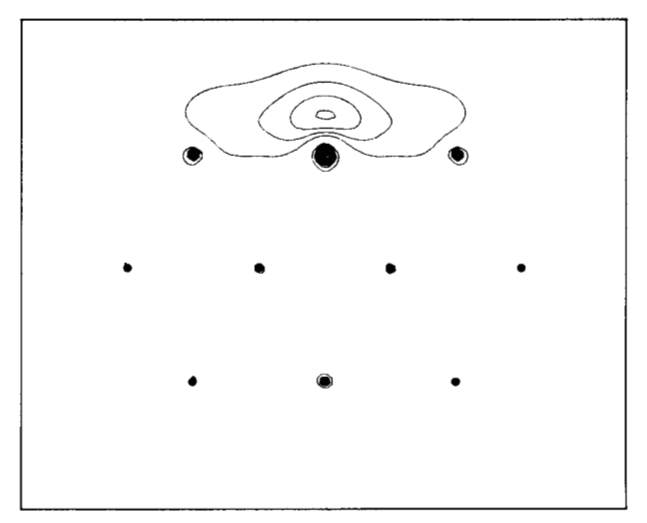


Figure 3 Contour plot of the orbital density of the singly-occupied 17a' SCF MO for the ³A' state of Be₁₃(10,3)A. The plane of the plot and the contour values are the same as in Fig. 2.

trarily large size. In any case, it is clear that we cannot use our calculated ΔST as a measure of the "bulk" behavior of the cluster.

For $Be_{14}(14,0)$ and $Be_{22}(14,8)$, we used a different approach to examine the energies of excited states of the cluster. The closed-shell-state orbitals, both occupied and unoccupied (virtual), were used to construct wave functions for the excited states. Double-open-shell configurations were formed by making excitations from the highest

Table 7 The energies of double-open-shell excited states of Be_{22} and Be_{14} obtained by using a frozen orbital approximation, as described in the text.

Cluster	State	Lowest excitation energy (eV)	Number of excited states within I eV of first excited state
	¹A′	1.29	9
Be ₂₂ (14,8)	¹ A"	1.48	12
	3 A $^\prime$	0.76	9
	³ A"	0.96	9
	¹ A′	1.27	3
D - (14.0)	¹A"	0.07	1
$Be_{14}(14,0)$	3 A $^\prime$	1.18	5
	3 A"	-0.07	2

occupied orbitals into low-lying virtual orbitals. Slater determinants were combined to form singlet and triplet spin functions. The procedure is described in detail in Section 3B. We hoped to avoid or reduce the problem described above (differential edge effects obtained from separate SCF calculations on the closed- and open-shell states) by using a common set of orbitals determined for the closed-shell state. The energies of these open-shell states are summarized in Table 7. We report the energies (relative to the closed-shell state) of the lowest open-shell state of each symmetry, ¹A', ³A', ¹A'', and ³A''. We also report the number of open-shell states within 1 eV above the lowest state of each symmetry.

The low energies of the $^{1}A''$ and $^{3}A''$ states for Be $_{14}$ are a feature of that particular cluster since such low energies are not obtained for Be $_{22}$. For Be $_{22}$, the excitation energies are reasonably large, ≈ 1 eV, and the separation of singlet and triplet states is also large, ≈ 0.5 eV. Thus, with this model, Be $_{22}$ is not large enough to show metallic character. However, the number of low-lying excited states is larger for Be $_{22}$ than for Be $_{14}$. In particular, the increase in the number of low-lying states is much larger than the increase in the number of atoms in the cluster. By this measure, Be $_{22}$ is beginning to show "bulk" character.

The next bare-cluster property considered is the first ionization potential IP. The IP of Be_n is defined as the difference of the SCF energies of the lowest closed-shell state of Be_n and the lowest single-open-shell doublet state of Be_n^+ (separate variational calculations are performed). The values of the IP are tabulated in Table 7. If, for the larger clusters, the IP resulted from removal of charge from the interior atoms, it would be appropriate to compare the IP to a "bulk" work function. From Table 6, it is seen that the IP for the larger clusters appear to be converging toward a value near 5 eV. It is tempting to believe that this value is one characteristic of a work function for infinite one- or two-layer systems.

In Table 8, we give for our largest cluster [Be₂₂(14,8)], the charges on each atom, $Q_{\rm A}$ (given in units of electron charge e; $1~e=1.602\times 10^{-19}$ coulombs), for the neutral cluster and for the ion. The charges are determined from a Mulliken gross population analysis [46]. The difference $\Delta Q_{\rm A} = Q_{\rm A}({\rm Be}_{22}) - Q_{\rm A}({\rm Be}_{22}^+)$ is a measure of the charge removed from each atom upon ionization. If charge were removed uniformly from all 22 atoms, each ΔQ_{Δ} would be 0.045 e. The five interior atoms of the Be₂₂ cluster (11–14 and h in Fig. 1) would lose a total of 0.23 e. However, three of these five atoms (11, 13, and g) actually have larger charges in the ion than in the neutral cluster (ΔQ_{Δ} < 0). The sum of the ΔQ_{Δ} for the five interior atoms is such that they gain 0.01 e. The gain of atomic charge in the ion is possible because the separate SCF calculation for Be₂₂ allows the charge distribution to reorganize (relax) in response to the removal of an electron [47]. The Be, ion is formed by removing an electron from the 27a' orbital. The atomic populations [46] of this orbital for the SCF wave function for neutral Be₂₂, $Q_{\Delta}(27a'; Be_{22})$, are also given in Table 8. These values correspond to $\Delta Q_{\rm A}$ for the unrelaxed ionic wave function where the MOs are not allowed to reorganize. They are quite different from the $\Delta Q_{\rm A}$. Clearly, reorganization effects characteristic of localized behavior are important in the ionization of Be₂₀. Another measure of reorganization is the relaxation energy [47] (the difference between the Koopmans' Theorem IP and the \triangle SCF value reported in Table 7). For Be₂₀, this relaxation energy is 0.7 eV.

The key conclusion to be drawn is that in forming Be_{22}^+ the electron is, in essence, removed entirely from edge atoms. Thus, it is clear that the Be_{22} IP is not at all characteristic of a "bulk" work function value. The IP for large finite one- and two-layer clusters may, in fact, converge to a value of ≈ 5 eV. However, it is possible that it will also continue to involve the removal of the electron from edge atoms.

The cohesive energy $E_{\rm coh}$ of a ${\rm Be}_n$ cluster is defined as the binding energy per atom. It is represented by

$$E_{\text{coh}} = [E_{\text{SCF}} (\text{Be}_n) - nE_{\text{SCF}} (\text{Be atom})]/n.$$
 (6)

Values of $E_{\rm coh}$ for the various clusters are also given in Table 6. It is clear that these values are by no means converged; nor are they even close to the 78 kcal/mol (3.27 \times 10⁵ J/mol) cohesive energy of Be metal [48]. This is hardly surprising.

A measure of edge effects in the ground state charge distribution of Be₂₂ may be obtained from the population analysis [46] of the valence electrons. We define the valence population on an atom to be the total population less two 1s electrons. The remaining population is assigned as 2s or 2p. This population decomposition is given in Table 9. For a semi-infinite surface, all first-layer atoms must be equivalent. The interior atoms in the first layer of

Table 8 Gross atomic charges Q_A in units of electron charge e for Be_{22} and Be_{22}^+ . The interior atoms are listed first.

Atom number	$Q_{A}(Be_{22})$	$Q_{\mathrm{A}}(\mathrm{Be}_{22}^+)$	$\Delta Q_{ m A}$	$Q_{\rm A}(27{\rm a'};{\rm Be}_{22})$
11	3.981	4.028	-0.048	0.051
12 or 14	4.027	4.002	+0.025	0.068
13	4.030	4.037	-0.007	0.020
h	3.998	4.006	-0.008	0.030
1 or 10	3.983	3.879	+0.104	0.082
2 or 9	4.037	3.975	+0.062	0.035
3 or 8	3.937	3.872	+0.066	0.039
4 or 7	4.048	3.990	+0.057	0.082
5 or 6	3.971	3.897	+0.074	0.061
a or g	4.010	3.985	+0.024	0.033
b or f	3.979	3.911	+0.068	0.023
c or e	4.019	3.996	+0.022	0.012
d	3.971	3.914	+0.056	0.033

the Be₂₂ cluster (11 to 14) do, in fact, have very similar valence populations; ≈ 0.6 2s and ≈ 1.4 2p electrons. Their hybridization is very different from those of the exterior atoms. Atom h, the interior atom in the second layer, is much closer in hybridization to the other interior atoms than to that of the exterior atoms. Thus, the Be₃₀ cluster may well be large enough to contain interior atoms with charge distributions characteristic of those which would be found for a semi-infinite surface. This is of particular importance for the ability of the cluster to give meaningful results for the chemisorption process. The interior atoms form the sites at which we have added the adsorbed H atom to Be₂₂. It is clear from Table 9 that sites involving exterior atoms would not be satisfactory. With many of the smaller clusters used in our previous work [21, 24], we were forced to use such sites.

We have shown that the singlet-triplet splittings ΔST and the IP are best viewed as reflecting edge behavior in the clusters. The clusters are also far too small to give a converged behavior for $E_{\rm coh}$. However, the ground state population analysis indicates that the interior atoms of Be₂₂ are likely to be sufficiently free from edge effects to form suitable sites for the study of chemisorption.

5. Results: clusters with H

For each of the Be_n clusters a hydrogen atom was added in one or more of the four chemisorption sites described in Section 2. (The specific geometries of the sites used are described in Appendix A.) The SCF energy of Be_n-H was computed for several different vertical distances of H from the "surface" of Be_n in order to obtain a potential interaction curve. The spacing between adjacent points was 0.1 a_0 (Bohr radius; $1a_0 = 5.29 \times 10^{-2}$ nm). The distances were chosen in order to bracket the minimum of the potential curve and the three points about the minimum were fit to a quadratic polynomial. The equilibrium

Table 9 Decomposition of the valence electron gross atomic populations of Be₂₂ into 2s and 2p character. The interior atoms are listed first.

Atom number	2s Population	2p Population	Total valence population
11	0.59	1.39	1.98
12 or 14	0.61	1.42	2.03
13	0.63	1.40	2.03
h	0.52	1.47	2.00
1 or 10	0.90	1.08	1.98
2 or 9	0.70	1.33	2.04
3 or 8	0.92	1.02	1.94
4 or 7	0.80	1.25	2.05
5 or 6	0.92	1.05	1.97
a or g	0.76	1.25	2.01
b or f	0.75	1.23	1.98
c or e	0.67	1.35	2.02
d	0.93	1.04	1.97

hydrogen distance (position of the interpolated minimum) $r_{\rm e}$ and the dissociation energy (or chemisorption bond energy) $D_{\rm e}$ were computed. The $D_{\rm e}$ are defined as the interpolated depth of the curve with respect to the SCF energies of separated Be_n and H. In this section we focus on these two properties of the Be_n-H clusters. We also consider Mulliken population analyses [46] of the charge distributions for Be₂₂-H in order to examine the nature of the substrate-hydrogen bond. As in the previous section, an important concern is with the identification and measurement of edge effects and convergence of the calculated chemisorption properties.

In Table 10, we give a complete summary of the calculated values for $r_{\rm e}$ and $D_{\rm e}$. A careful comparison of Tables 6 and 10 shows that no simple correlation exists which connects any of the bare cluster properties with the chemisorptive properties. This lack of correlation is easily un-

Table 10 Summary of the values of r_e (nm) and D_e [kcal/mol; J/mol (10⁵)] for the various Be_n-H clusters and adsorption sites. The results given were obtained using minimum basis sets as described in Section 3D.

Site	Model	r _e (nm)	$D_{\rm e}$
			[kcal/mol; J/mol (10 ⁵)]
Open	$Be_3(3,0)$	0.125	19.1; 0.80
•	$Be_6(6,0)$	0.118	47.3; 1.98
	$Be_{14}(14,0)$	0.111	56.1; 2.35
	$Be_5(4,1)$	0.102	23.2; 0.97
	$Be_6(3,3)$	0.111	55.3; 2.32
	$Be_{9}(6,3)$	0.113	50.2; 2.10
	$Be_{13}(10,3)A$	0.099	39.0; 1.63
	$Be_{22}(14.8)$	0.094	55.1; 2.31
Eclipsed	$Be_4(3,1)$	0.124	28.7; 1.20
	$Be_{5}(4,1)$	0.115	30.1; 1.26
	$Be_{7}(6,1)$	0.111	40.8; 1.71
	$Be_{13}(10,3)A$	0.090	57.2; 2.40
	$Be_{13}(10,3)B$	0.094	58.3; 2.44
	$Be_{22}(14,8)$	0.097	51.9; 2.17
Bond midpoint	$Be_4(4,0)$	0.126	70.1; 2.94
	$Be_{10}(10,0)$	0.117	45.3; 1.90
	$Be_{14}(14,0)$	0.017	53.1; 2.22
	$Be_5(4,1)$	0.114	32.4; 1.36
	$Be_{13}(10,3)$	0.105	44.8; 1.88
	$Be_{22}(14.8)$	0.104	53.4; 2.24
Directly	$Be_1(1,0)$	0.142	46.4; 1.94
overhead	$Be_7(7,0)$	0.143	71.3; 2.99
	$Be_{14}(14,0)$	0.140	59.0; 2.47
	$Be_{10}(7,3)$	0.143	27.3; 1.14
	$Be_{13}(10,3)$	0.141	31.1; 1.30
	$Be_{22}(14,8)$	0.139	31.4; 1.32

derstandable. The cluster properties are affected by the cumulative edge effects. However, we expect the chemisorption properties to be determined primarily by the interaction of the H adatom with its nearest surface neighbors. Only those edge effects that influence the charge distribution about these substrate bonding Be atoms will strongly affect the chemisorption results. Thus, edge effects measured by the bare cluster properties do not simply or directly correlate with those that are important for chemisorption. As we shall see below, much more careful and detailed analyses are required.

Before we continue with the analysis of the convergence of $r_{\rm e}$ and $D_{\rm e}$, we will present some features of the charge distribution and wave functions of ${\rm Be}_{22}$ -H. We consider the ${\rm Be}_{22}$ -H results at the calculated point closest to the minimum of the interaction potential: $r=1.8~a_0$ for the open and eclipsed sites, $r=2.0~a_0$ for the bond midpoint site, and $r=2.6~a_0$ for the directly overhead site, where r is the distance of the H atom above the first ${\rm Be}_{22}$ layer. In Table 11, we give Mulliken gross population analyses for the bond midpoint site as a representative case; we give the total charge per atom, $Q_{\rm A}$ (in e), and the difference of the populations with ${\rm Be}_{22}$, $\Delta Q_{\rm A}=$

 $Q_A(Be_{22}-H) - Q_A(Be_{22})$. The Q_A for $Be_{22}-H$ are reasonably close to four for each Be atom, suggesting that edge effects on the gross distribution of charge are not large. The Q_{Λ} of H is only slightly different from 1e and the ΔQ_{Λ} for the Be atoms are fairly small, the largest value (for atom h) being 0.05e. Both of these features are suggestive of covalent bonding of the H to the Be cluster and of the relative unimportance of edge effects. The population analysis for the open (singly-occupied) shell of Be₂₂-H, $Q_{\rm A}(28{\rm a}')$, gives a different impression of the importance of edge effects. As shown in Table 11, this MO is quite localized: 84 percent of the charge is on edge atoms 1 and 10 (cf. Fig. 1). Thus, although the total charge is rather uniformly distributed over the Be22 cluster, the spin density shows strong edge effects. A consequence of this localization may be seen in the Be22-H bond midpoint valence shell orbital energies given in Table 12. The openshell $\varepsilon(28a')$ lies considerably lower than the ε of the closed-shell-valence MOs. It is 2.15 eV lower in energy than $\varepsilon(27a')$ [49]. The reason for the localization of the 28a' MO follows from restricted Hartree-Fock MO theory [50]. The closed-shell orbitals all have a self-coulomb interaction. Since this repulsive interaction is large for localized MOs, the closed shells tend to be delocalized over the cluster. The open-shell orbital does not have this interaction and can gain nuclear attraction energy by localizing. If the orbital energy is a guide to the energetic consequences of localization, then the D_e is uncertain by \approx 2 eV or \approx 45 kcal/mol (\approx 1.9 \times 10⁵ J/mol), which is as large as the computed D_e .

This is, however, likely to be a gross overestimate since the total energy of Be,,-H can be expected to depend more strongly on the spin-independent coulomb interactions than on the smaller spin-dependent exchange interactions [40]. In order to obtain a more reliable estimate of the effects of having a strongly localized openshell MO, we performed an SCF calculation for the closed-shell positive ion Be₂₂-H⁺, at the bond midpoint site. The closed-shell MOs of the ion, together with the virtual 28a' MO, $\varphi_v(28a')$, were used to construct a wave function for Be₂₂-H. The population analysis for this Be₂₂-H wave function and for $\varphi_{v}(28a')$ are given in Table 13. Unlike the localized occupied open-shell 28a' MO, $\varphi_{v}(28a')$ is delocalized over the entire cluster. However, the energy obtained with this wave function is only 0.57 eV [or 13 kcal/mol (2.4×10^3 J/mol)] higher than the Be,,-H SCF energy. Since some relaxation effects are to be expected for a finite cluster, it seems reasonable to estimate that the uncertainty in D_{e} associated with the localized behavior of the open-shell MO is about half of this $(\approx 1.2 \times 10^3 \text{ J/mol})$. This is an acceptably small value.

Another indication that the edge effects are reasonably small may be seen in the local symmetry of the Be-H overlap populations for the bond midpoint, open, and

Table 11 Gross atomic charges Q_A in units of electric charge e for the bond midpoint site of Be₂₂-H and for Be₂₂.

Atom number	$Q_{A}(Be_{22}-H)$	$Q_{\mathrm{A}}(\mathrm{Be}_{22})$	$\Delta Q_{\mathtt{A}}$	$Q_{\rm A}(28{\rm a'})$
11	3,989	3.981	+0.008	0.019
12 or 14	4.062	4.027	+0.035	0.003
13	3.994	4.030	-0.036	0.002
h	4.052	3.998	+0.054	0.012
1 or 10	3.958	3.983	-0.025	0.410
2 or 9	4.007	4.037	-0.030	0.006
3 or 8	3.947	3.937	+0.010	0.003
4 or 7	4.018	4.048	-0.030	0.004
5 or 6	3.973	3.971	+0.002	0.004
a or g	4.025	4.010	+0.015	0.026
b or f	3.974	3.979	-0.005	0.017
c or e	4.040	4.019	+0.021	0.009
d	3.949	3.971	-0.022	0.002
Н	1.009		1.009	0.001

eclipsed sites. For a sufficiently large cluster, the overlap populations of H with the nearest-neighbor substrate atoms must be equal. These populations are given in Table 14; for the bond midpoint site, we include the second-nearest-neighbor Be atoms (11 and 13) as well. For all other sites, the overlap with second nearest neighbors is negligibly small. The equality of the H-12 with the H-14 overlap population is imposed by the C_s symmetry of the Be₂₀-H cluster. The near equality of H-11 with H-12 for the eclipsed site and H-13 with H-12 for the open site are consequences of the size of the cluster. In the worst case (eclipsed site) these differ by only 16 percent. For the bond midpoint site, the small next-nearest-neighbor overlap populations H-11 and H-13 are not too different from each other. These results support the belief that there are a sufficient number of interior atoms in the Be,, cluster to accurately describe chemisorption without serious consequences from edge effects.

The nature of the bonding of H to the Be surface can also be considered by examining the decomposition of the valence shell population analysis into 2s and 2p character. In Table 15, this decomposition is given for the Be atoms nearest to the H. For each adsorption site, the amount of 2p character of these bonding Be atoms increases over that found for the bare Be₂₂ cluster. This is reasonable since the 2p can provide directional character needed for bonding with H. The increase is most marked for the directly overhead site, which requires substantial p₂ character to form the one Be-H bond. We also note that for the threefold sites the populations on all three "equivalent" bonding Be atoms are rather similar. For all sites, the H atom population is nearly characteristic of covalent bonding.

We now return to a comparison of the computed values for $D_{\rm e}$ and $r_{\rm e}$ for the various clusters (cf. Table 10). Each of the four sites is considered separately as follows.

Table 12 Valence shell orbital energies ε for the bond midpoint site of Be₂₂-H. The 28a' MO is the open-shell orbital.

na'	ε (hartree; eV)	na"	ε (hartree; eV)
14	-0.699; -19.02	10	-0.586; -15.95
15	-0.623; -16.95	11	-0.487; -13.25
16	-0.555; -15.10	12	-0.398; -10.83
17	-0.517; -14.07	13	-0.347; -9.44
18	-0.462; -12.57	14	-0.290; -7.89
19	-0.438; -11.92	15	-0.264; -7.18
20	-0.372; -10.12	16	-0.222; -6.04
21	-0.331; -9.01	17	-0.214; -5.82
22	-0.303; -8.25		,
23	-0.299; -8.14		
24	-0.268; -7.29		
25	-0.233; -6.34		
26	-0.218; -5.93		
27	-0.202; -5.50		
28	-0.281; -7.65		

Table 13 Gross atomic charges in units of electron charge e for a wave function for the bond midpoint site of Be₂₂-H constructed from the occupied and 28a' virtual SCF MOs of the closed-shell positive ion Be₂₂-H⁺. The atomic charges of the 28a' virtual MO are given separately.

Atom number	$Q_{A}(Be_{22}\text{-}H)$	$Q_{\rm A}(28a', virtual MO)$
11	3.959	0.033
12 or 14	4.097	0.016
13	3.990	0.031
h	4.064	0.037
1 or 10	3.984	0.098
2 or 8	3.993	0.018
3 or 8	3.917	0.045
4 or 7	4.032	0.070
5 or 6	3.966	0.060
a or g	4.008	0.035
b or f	3.991	0.058
c or e	4.051	0.035
d	3.909	0.023
Н	0.996	0.006

Table 14 Overlap populations between H and the nearest neighbor Be atoms for the bond midpoint, open, and eclipsed sites of Be_{22} -H. For the bond midpoint site, overlap populations are also given for the next nearest Be atoms.

	Overlap populations		
	H-11	H-12 or H-14	H-13
Bond midpoint	0.018	0,409	0.013
Open	_	0.310	0.278
Eclipsed	0.267	0.317	

Table 15 Decomposition of the valence electron atomic populations of the bonding Be atoms, for all four adsorption sites for H on Be₂₂, into 2s and 2p character. The values for the bare Be₂₂ cluster are included for comparison.

		Atom 11	Atoms 12 or 14	Atom 13	Н
	s	0.59	0.61	0.63	
Be_{22}	р	1.39	1.42	1.40	
	total	1.98	2.03	2.03	
David	s	_	0.56	_	1.01
Bond	p		1.50		
midpoint	total		2.06		1.01
	s	_	0.56	0.59	1.02
Open	p	_	1.46	1.48	
_	total	_	2.02	2.07	1.02
	s	0.57	0.57		1.02
Eclipsed	p	1.49	1.45	_	
-	total	2.06	2.02	_	1.02
T	s	0.58		_	0.96
Directly	р	1.73			
overhead	total	2.30		_	0.96

Table 16 Distance, in nm, of the H atom from various Be atoms surface for all four adsorption sites considered. The vertical distance from the surface is the $r_{\rm e}$ calculated for the Be₂₂-H clusters.

Distance		Site		
	Directly overhead	Bond midpoint	Open	Eclipsed
Vertical (r _e)	0.139	0.104	0.094	0.097
Nearest neighbor (first layer)	0.139	0.155	0.162	0.164
Next nearest neighbor (first layer)	0.268	0.224	0.280	0.281
Next nearest neighbor (second layer)	0.344	0.291	0.303	0.276

- 1. Directly overhead site. The results for the largest twolayer clusters, Be, (10,3)B and Be, (14,8), are quite similar to each other. Since, for both of these clusters, the bonding Be atom is in the interior of the cluster, it is reasonable to take $r_e = 0.14$ nm and $D_e \approx 30$ kcal/ mol $(1.3 \times 10^5 \text{ J/mol})$ as converged values for this site. For all clusters, including the Be atom [Be₁(1,0)], the $r_{\rm o}$ are about the same. This suggests that the bonding is similar in every cluster. The larger changes in D_{e} among the clusters may be ascribed to edge effects. The D_0 for the one-layer Be₁₄(14,0) and two-layer Be₁₄(14,8) clusters are quite different; for Be₁₄ the D_e is larger by about a factor of two. This is quite unlike the results for the bond midpoint and open sites where the D_{e} for Be₁₄ and Be₂₂ are extremely close to each other. We speculate that this is because of a large p, character in the directly overhead Be-H bond. The increased p, character in the bond will reduce the bonding between the two Be layers and hence reduce $D_{\rm e}$ for the two-layer cluster. Preliminary results for a threelayer Be₃₆(14,8,14) cluster also give $\approx 1.3 \times 10^5$ J/mol for D_o .
- 2. Bond midpoint site. The $D_{\rm e}$ for the largest two-layer clusters, ${\rm Be_{13}(10,3)A}$ and ${\rm Be_{22}(14,8)}$, differ by ≈ 9 kcal/mol (3.8 \times 10⁴ J/mol). Thus, for this site both the next-nearest Be neighbors and the nearest neighbors to the adsorbed H should also be interior atoms (as is the case in ${\rm Be_{22}}$, but not in ${\rm Be_{13}}$). In Table 16, we give vertical ($r_{\rm e}$), nearest-neighbor, and next-nearest-neighbor distances from H for each site on ${\rm Be_{22}}$. For the bond midpoint site, the distance between H and the next-nearest neighbors is fairly short and the overlap populations (Table 14) are small but non-negligible. Thus, the next-nearest neighbors should be more important for this site than for any other.

The D_e value for the one-layer Be₁₄(14,0) cluster is almost identical to that for the two-layer Be₉₉(14,8) cluster. The $r_{\rm e}$ value for Be₁₄ is approximately ten percent larger than that for Be₂₂. Further, as we show in the next section, the curvature of the interaction potential (force constant) is almost the same for Be₁₄ and Be₂₂. The one-layer and two-layer results are rather similar. This may be because much less p, character is required to form the Be-H bond for this site than for the directly overhead site. (For this site, the Be-H bond is directed at an angle of 42° to the surface for the Be₃₀-H cluster; for the directly overhead site, the bond angle is 90°.) Thus, the bonding of the top layer with the second layer will be less modified by the bonding of the nearest-neighbor Be atoms with H and the one- and two-layer D_e values will be similar. This argument is supported by the fact that the increase of the 2p character of the nearest-neighbor Be atoms when the H atom is added (cf. Table 15) is much less for this site

- than for the directly overhead site. The decrease in $r_{\rm e}$ from Be₁₄(14,0) to Be₂₂(14,8) corresponds to a decrease of bond angle from 46 to 42°. The smaller bond angle for the two-layer cluster means that less p_z character is required to form the Be-H bond.
- 3. Open site. The $D_{\rm e}$ for the largest two-layer clusters, Be₁₃(10,3)A and Be₂₂(14,8), are different by \approx 16 kcal/mol (6.7 \times 10⁴ J/mol) or \approx 30 percent; the $r_{\rm e}$ differ by 5 percent. This is not surprising since all the bonding (nearest-neighbor) Be atoms are not interior atoms for Be₁₃. The behavior of the $D_{\rm e}$ and $r_{\rm e}$ for Be₁₄(14,0) and Be₂₂(14,8) are very similar to that for the bond midpoint site. The same explanations for the behavior apply to this site.
- 4. Eclipsed site. As for the open site, $D_{\rm e}$ for Be₂₂(14,8) is fairly different from the values for the next-largest cluster (Be₁₃). Again, it is only for the Be₂₂ cluster that all the bonding Be atoms are also interior atoms.

We may summarize by recalling that all of the considerations put forward argue for a local nature for the Be-H bonding. However, $D_{\rm e}$ and $r_{\rm e}$ may well be affected by modification of the bonding between layers of the cluster, which results as a consequence of the bonding to H. It is tempting to conclude that $D_{\rm e}$ and $r_{\rm e}$ will be fairly well converged for any given site when all the bonding surface atoms are in the interior of the cluster. This convergence has, however, only been shown for the directly overhead site. It is difficult to estimate accurately the consequences of edge effects on $D_{\rm e}$ and $r_{\rm e}$. However, the calculations using Be $_{22}$ H $^+$ orbitals do suggest that, for the Be $_{22}$ cluster, edge effects will (reasonably) only introduce an uncertainty of \approx 6 kcal/mol (1.2 \times 10 3 J/mol) in $D_{\rm e}$.

Lavery and Hillier [51] have studied the adsorption of both H atoms and H, molecules on Be(0001). They used a tight-binding crystal orbital method that permitted them to consider infinite two-dimensional arrays of adsorbate on as many as three layers of substrate Be atoms. The matrix elements for the tight-binding Hartree-Fock matrix were approximated by completely neglecting differential overlap [52]; the authors described the approach as semi-empirical. For adsorption of an atomic overlayer on all possible threefold sites (both open and eclipsed), large differences were found between the results for one layer of Be and those for two layers of Be atoms. For three layers, they reported essentially the same results as for two layers. The D_{\circ} value for a one-layer substrate was given as 67 kcal/mol (2.81 \times 10⁵ J/mol) and was reduced to 39 kcal/mol (1.63 \times 10⁵ J/mol) for two layers. Our D_0 values for the open and eclipsed sites are nearly the same for Be₁₄(14,0) and Be₂₂(14,8). Lavery and Hillier found that $r_{\rm e}$ increased by approximately ten percent in going from one layer to two layers; we find a decrease of about

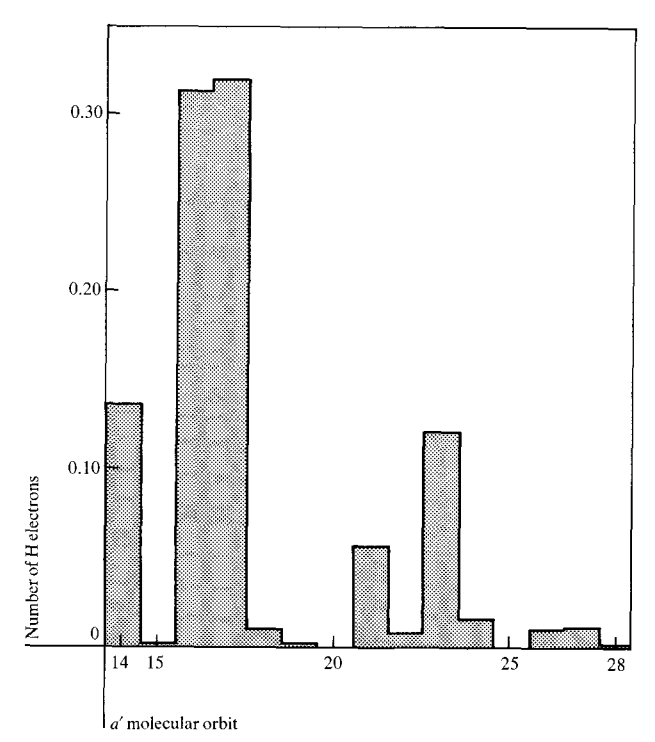


Figure 4 The fractional number of H electrons in each valence MO of a' symmetry for the bond midpoint site of Be_{22} -H. The orbital energies for this case are given in Table 13.

ten percent. They also studied monolayer adsorption at directly overhead sites but only for a one-layer substrate, and found a $D_{\rm e}$ of 31 kcal/mol (1.3 × 10⁵ J/mol). This is exactly our result for the two-layer clusters. In every case, their results and trends are different from ours. It is not likely that their semi-empirical method can describe chemisorption of H on a metal surface. Their results for H_2 adsorption cast further doubt on the utility of the method. They find that H_2 is molecularly chemisorbed with binding energies between 2.3 and 3.0 eV, depending on the site. With this large a binding energy, H_2 would be expected to easily adsorb on Be(0001). However, Adams [32(a)] and Hurd and Adams [32(b)] have reported that H_2 was not adsorbed either on Be films or on the (0001) face of a Be crystal.

The adsorption of H on metal surfaces has also been treated theoretically by using a jellium model for the metal substrate [53, 54]. Lang and Williams [53], for a high-density metal substrate with electronic radius $r_{\rm s}=2~a_{\rm o}$ (for Be, $r_{\rm s}=1.88$ [55]), find $D_{\rm e}=35$ kcal/mol (1.47 × 10^5 J/mol) Wang and Weinberg [54], with an $r_{\rm s}$ suitable to Be, find $D_{\rm e}=50$ kcal/mol (2.10 × 10^5 J/mol). Since jellium models cannot take account of the differences among adsorption sites, these values, in particular those of Wang and Weinberg [54], may be regarded as being reasonably close to our results for Be $_{22}$ -H.

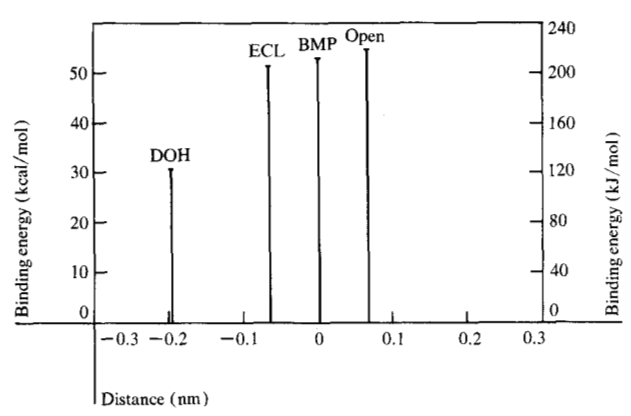


Figure 5 Binding energies of H on Be₂₂ at the directly overhead (DOH), eclipsed (ECL), bond midpoint (BMP), and open sites. The energies are shown along the line connecting the four sites and passing through atoms 11 and 13 of the cluster. The origin is placed at the midpoint of atoms 12 and 14 (see Fig. 1).

Finally, it seems worthwhile to indicate how the H atom population is distributed over the Be_n -H MOs. Consider for example the bond midpoint site for Be_{22} -H. Figure 4 is a histogram showing the (fractional) number of H electrons in each valence MO of a' symmetry as given by a Mulliken gross population analysis [46]. (The H population of the a'' MOs is zero by symmetry considerations.) The hydrogen population is mostly in those orbitals with approximately the same orbital energy as the free hydrogen orbital, -0.5 hartree (13.606 eV). Orbitals 16a' and 17a' have orbital energies of -0.56 hartree and -0.52 hartree (cf. Table 12) and together they contain 63 percent of the hydrogen population.

6. Chemisorption of H

In this section, we apply the results described in the previous sections to the analysis of various aspects of the chemisorption of H on Be(0001). The results for $D_{\rm e}$ and $r_{\rm e}$ for the four sites treated are summarized and some consequences for coverage dependence of the adsorption energy and the dissociative adsorption of H_2 are described. A simple model for the incorporation of H into the bulk of Be is also considered. Finally, vibrational energies for the motion of the H normal to the surface are presented and the dependence of these energies on the adsorption site coordination is analyzed. Our results for Be are compared to electron energy loss (EEL) [56] measurements of surface vibrations for H on W(100).

From the discussion in the previous section, it seems reasonable to assume that the Be_{22} cluster is large enough to describe the bonding at all four chemisorption sites with nearly equal accuracy. We may summarize the results for the binding energy and equilibrium bond length by recalling that three sites (bond midpoint, open, and eclipsed) have rather similar values; $D_e \approx 50$ kcal/mol

 $(2.1 \times 10^5 \text{ J/mol})$ and $r_e \approx 0.1 \text{ nm}$. The fourth site, directly overhead, is substantially different, having $D_e \approx$ 30 kcal/mol (1.3 \times 10⁵ J/mol) and $r_e \approx 0.14$ nm. Further, for this last site, the one- [Be₁₄(14,0)] and two-[Be₉₉(14,8)] layer clusters gave very different values for $D_{\rm e}$. The one-and two-layer $D_{\rm e}$ values for the other sites were rather close to each other. We have interpreted this as being due to the larger involvement of p_z character for bonding at the directly overhead site than at the other sites. The bonding to H does not differ significantly between the one- and two-layer clusters. However, for the two-layer cluster, the p, character required for bonding between the two substrate layers is reduced in order to form the Be-H bond. This results in an increase of the total energy of the system of adsorbate plus adatom because the substrate is now more weakly bound together. This reasoning suggests that the binding energy of H in the directly overhead site may be significantly coverage dependent. As more H atoms are added at these sites, the p, character required for bonding the first to the second substrate layer will become more depleted. Thus, the binding energy per adatom would become smaller with increasing coverage. It is interesting to note that this analysis is consistent with the behavior observed by EEL spectroscopy for H on W(100) [56]. Here, the adsorption at low coverage is ascribed only to directly overhead sites. At higher coverages, H begins to adsorb at bridge (bond midpoint) sites as well as at the directly overhead site. At full coverage, adsorption is exclusively at the bridge site.

The calculated binding energies of two H atoms adsorbed at some combination of bond midpoint, open, and eclipsed sites is 104-110 kcal/mol (4.4-4.6 \times 10⁵ J/mol). This is only slightly smaller than the dissociation energy of the H_a molecule [57]; $D_a(H_a)$, ≈ 109.5 kcal/mol (4.6 × 10° J/mol). The basis set tests described in Section 3A indicate that the minimum basis set D_e is most likely to be smaller than the double zeta basis set value. Moreover, SCF calculations usually give a value of D_a that is smaller than the experimental value [2]. Thus, it is reasonable to expect that the dissociative adsorption of H, will be exothermic. In Fig. 5, we show the variation of the calculated H binding energy on Be₂₂ as a function of site along the line connecting the four adsorption sites. This line (the x axis of the cluster) passes through atoms 11 and 13 (see Fig. 1). It is quite possible that there is a relatively flat attractive portion of the interaction potential along this line between the eclipsed and open sites. If so, an H_o molecule could approach the surface and dissociate into two adsorbed H atoms at nearly (adjacent) high binding energy sites. Of course, this analysis is oversimplified. It does not take into account a potential barrier for the breaking of the H₂ bond or a change in D_e when H atoms are adsorbed at nearby sites.

Since hydrogen is known [58] to be *absorbed* into the bulk for many metals, this possibility was considered for the open site of Be_{22} -H: When the H atom is placed on the surface (r=0.00 nm) the energy is only 4 kcal/mol (1.7 × 10^4 J/mol) below the asymptotic limit of Be_{22} plus H. When the H is halfway between the top and bottom layers (r=-0.09 nm) the system has a total energy only 2 kcal/mol (8.4 × 10^3 J/mol) below this limit, and is 53 kcal/mol (2.22 × 10^5 J/mol) above the chemisorbed equilibrium value. The total energy appears to become continuously higher as r is decreased from its equilibrium value, $r_{\rm e}=0.094$ nm. Thus it appears unlikely that absorption into a perfect beryllium crystal will occur without some deformation of the crystal structure.

For the Be₂₂(14,8) and the one-layer Be₁₄(14,0) clusters, the vibrational frequency of H for motion normal to the surface has been computed in order to investigate the site dependence of the surface vibrations. It is well known that the SCF method is able to provide reasonably accurate force constants [2]. A good rule for molecules is that the computed quadratic force constants are in error by ≈ 15 percent. Thus, if the Be_n cluster is sufficiently large to model the interaction of a surface with an adsorbed H atom, we may expect reasonable results for surface vibrations. To our knowledge, our results are the first calculations of vibrational energies that explicitly include the geometric structure of the substrate; other approaches have been based on jellium models [54].

For each site, the force constants were determined by fitting the three points of the Be_n -H interaction potential nearest the minimum (cf. Section 5) to a parabola. The mass of the cluster was assumed to be infinite. The results are reported in Table 17. The frequencies are quite similar for Be_{14} and Be_{22} ; larger differences between these two clusters were found for either D_e (directly overhead site) or r_e (bond midpoint, eclipsed, and open sites), cf. Table 10. Thus it would appear that the shape of the interaction potential is well determined by the first layer even though the binding energy and equilibrium geometry are not so well determined.

The frequencies are clearly dependent on the site coordination of the adsorbed H. It is largest for the directly overhead (onefold site) and smallest and about equal for the two threefold sites. Clearly the frequencies depend on the site coordination, since the amount that a bond is stretched is $\Delta z \cos \alpha$, where Δz is the vertical displacement and α is the angle between the bond and a line normal to the surface. However, as the numbers of bonds change, the strength of any bond may be expected to change as well. In order to analyze and separate these effects, we assume a model where the H atom is connected by springs of force constant k to its nearest-neighbor Be atoms. For any site, all k must be the same since the Be atoms are all equivalent. Then

Table 17 Vibrational frequencies, ω_e (in cm⁻¹), for H adsorbed on Be₂₂(14,8) or Be₁₄(14,0). Relative values of the effective bond force constants k_n are also given for Be₂₂.

Site	$\omega_{\rm e}({ m Be}_{22})$	ω _e (Be ₁₄)	$k_n(\mathrm{Be}_{22})$
Directly overhead	2060	1960	1
Bond midpoint	1360	1300	0.48
Open	1230	1150	0.34
Eclipsed	1220		0.35

$$\omega_{e}(n) = C \cos \alpha_{n} \sqrt{nk_{n}} , \qquad (7)$$

where n is the number of nearest neighbors for the site and C is simply a constant. The relative values of k_n are given in Table 17. Clearly the force constants are quite different for different sites. The relation $nk_n \approx 1$ holds although there is no obvious reason why this should be so.

These vibrational energies for motion normal to the surface are appropriate for comparison with the results of EEL spectroscopy. For low primary energy electrons, there will be a large cross section for inelastic loss only for normal vibrations [59]. Recently, Froitzheim et al. [56] have obtained EEL results for H adsorbed on W(100). They observed two losses (vibrational frequencies), one at 0.155 eV and a second at 0.130 eV. The high energy loss was ascribed to a directly overhead site and the low energy loss to a bridge (bond midpoint) site for the adsorbed H atom. In their analysis of the site dependence of the vibrational energies, Froitzheim et al. [56] made the assumption that the relation $nk_n = 1$ would hold. Our results, albeit for H on Be rather than on W, provide the first theoretical justification for making this assumption.

7. Conclusions

From the analysis given in Sections 4 and 5, we were able to draw several conclusions concerning both the nature of the chemisorption of H and the use of the cluster model. Even the largest bare cluster, Be,, did not have properties characteristic of a bulk metal. Further, properties which might be thought to measure bulk behavior, e.g., first ionization and first excitation energies, may in fact be characteristic of edge properties even for arbitrarily large clusters. However, the interaction of the H adatom with the Be substrate is determined in large measure by the bonding of the adatom to its nearest Be neighbors. Thus, we expect that properties associated with chemisorption will converge rapidly as a function of cluster size. Our analysis suggests that a cluster for which all the substrate atoms involved in the local bonding to the adsorbed H atom are interior atoms of the cluster will give reasonably

well converged results for bond energy and bond distance. Our largest cluster, $\mathrm{Be}_{22}(14.8)$, meets this requirement for all four sites considered. This is, of course, a rather large cluster. It is possible that such a large cluster is needed because for H on Be the D_{e} for the various sites are not very different from each other and also because of the special features of the covalent bonding in this system. For oxygen on Li(100), where the adsorbate bonding is ionic in character and the D_{e} and r_{e} for different sites are quite different, there is evidence that smaller clusters are satisfactory [60].

The bonding of H to Be(0001) is covalent. When H adsorbs on Be, the bonding Be atoms rehybridize to have added p character in order to facilitate bonding with the H. The rehybridization is particularly important for the directly overhead site where, we believe, it leads to a reduction of the bonding between the layers of the Be substrate. This may result in a large coverage dependence of the chemisorption energy for this site.

We find that, with the exception of the directly overhead site, the H bond energies and equilibrium bond distances are rather similar, being ≈ 50 kcal/mol $(2.1 \times 10^5 \text{ J/}$ mol) and ≈ 0.1 nm. For the directly overhead site, D_a is 30 kcal/mol (1.3 \times 10⁵ J/mol) and r_e is 0.14 nm. It is interesting to note that the calculated chemisorption energy value of 2.2×10^5 J/mol is similar to that for H on transition metals [1], where the energy is in the range 60-70 kcal/mol, even though Be has no d electrons. The calculated values for D_{ρ} are most probably too small due to the use of a minimum basis set (see Section 3) and to the errors of SCF wave functions. If the actual D_{α} are only slightly larger than our computed values, the dissociative adsorption of H, on Be(0001) will be exothermic. We have also modeled the diffusion of H into the Be lattice through the open site on Be₂₉(14,8) and find that it is energetically unfavorable.

The adsorption sites have very different vibrational frequencies for motion normal to the surface. The order of frequencies is ν (directly overhead) $>\nu$ (bond midpoint) $>\nu$ (open) $\approx\nu$ (eclipsed). We have analyzed our calculated frequencies using a spring and ball model. We find that the spring force constant for each Be-H bond is inversely proportional to the number of bonds.

Some of the most significant results of this work, however, do not depend on the particular system chosen for the calculation. A molecular orbital cluster model can be used to obtain a detailed and, we believe, reasonably accurate description of various aspects of the chemisorption of atoms on metal surfaces. Of particular importance is the fact that we have obtained properties which require a knowledge of the relative energies of the system with the adatom at different geometries. Such properties are quite difficult to obtain by other theoretical methods. The model system Be plus H was chosen to allow us to make

extensive studies of convergence patterns. The cluster sizes required for convergent results are fairly large. However, if model potentials for the core electrons as developed, for example, by Bonifacic and Huzinaga [61] and Melius et al. [62] are used, the methods described in this paper can be applied to heavy atom substrates, e.g., transition metal atoms.

Acknowledgments

The work of C. W. Bauschlicher and H. F. Schaefer III was supported by the U.S. Energy Research and Development Administration. Note: The work cited in this paper was performed while C. W. Bauschlicher was affiliated with the Lawrence Berkeley Laboratory, University of California, Berkeley.

Appendix A: Cluster geometries

In this appendix, we give figures showing models of the clusters used for the calculations reported in this paper. The chemisorption sites used for each cluster are also given. The bond distances and the (0001) surface geometry are given in Section 2. The atoms in each cluster are denoted by using numbers for the atoms in the first layer and letters for those in the second layer.

Figure A1(a) shows the Be₄(3,1) cluster; when the second-layer atom a is removed, this is a model for $Be_3(3,0)$. The threefold site (center of atoms 1, 2, and 3) is an open site in $Be_a(3,0)$ and an eclipsed site in $Be_a(3,1)$. Both $Be_3(3,0)$ -H and $Be_4(3,1)$ -H have C_{3y} symmetry. Figure A1(b) shows the $Be_{5}(4,1)$ cluster; the top layer alone is $Be_4(4,0)$. For Be_5 , the open (center of atoms 2, 3, and 4), eclipsed (center of atoms 1, 2, and 4), and bond midpoint (center of atoms 2 and 4) sites were all used; for Be₄ only the bond midpoint site was used. The symmetry of $Be_4(4,0)$ -H is C_{2v} ; that of $Be_5(4,1)$ -H is C_s . Figure A1(c) shows the $Be_{\tau}(6,1)$ and $Be_{\epsilon}(6,0)$ clusters. Only the threefold site formed by atoms 2, 4, and 6 was used. Both clusters with H have C_{3v} symmetry. Figure A1(d) shows the $Be_{q}(6,3)$ cluster; the $Be_{6}(3,3)$ cluster is formed by removing atoms 1, 3, and 5. The open site at the center of atoms 2, 4, and 6 was used. The Be₁₀(7,3) and Be₇(7,0) clusters are shown in Fig. A1(e). Only the directly overhead site above atom 7 was used. The two Be₁₃ clusters, $Be_{13}(10,3)A$ and $Be_{13}(10,3)B$, are shown in Figs. A1(f) and (g), respectively. In Be₁₃(10,3)A, the open site (center of atoms 7, 9, and 10), the eclipsed site (center of atoms 3, 9, and 10), and the bond midpoint site (center of atoms 9 and 10) were used. In Be₁₃(10,3)B, the eclipsed site at the center of atoms 3, 4, and 10, and the directly overhead site above atom 10 were used. In the $Be_{10}(10,0)$ cluster, formed by removing atoms a, b, and c from either Be₁₃ cluster, only the bond midpoint site noted above was used. The B₂₂(14,8) cluster is shown in Fig. 1 of the text; $Be_{14}(14,0)$ is the top layer of this cluster.

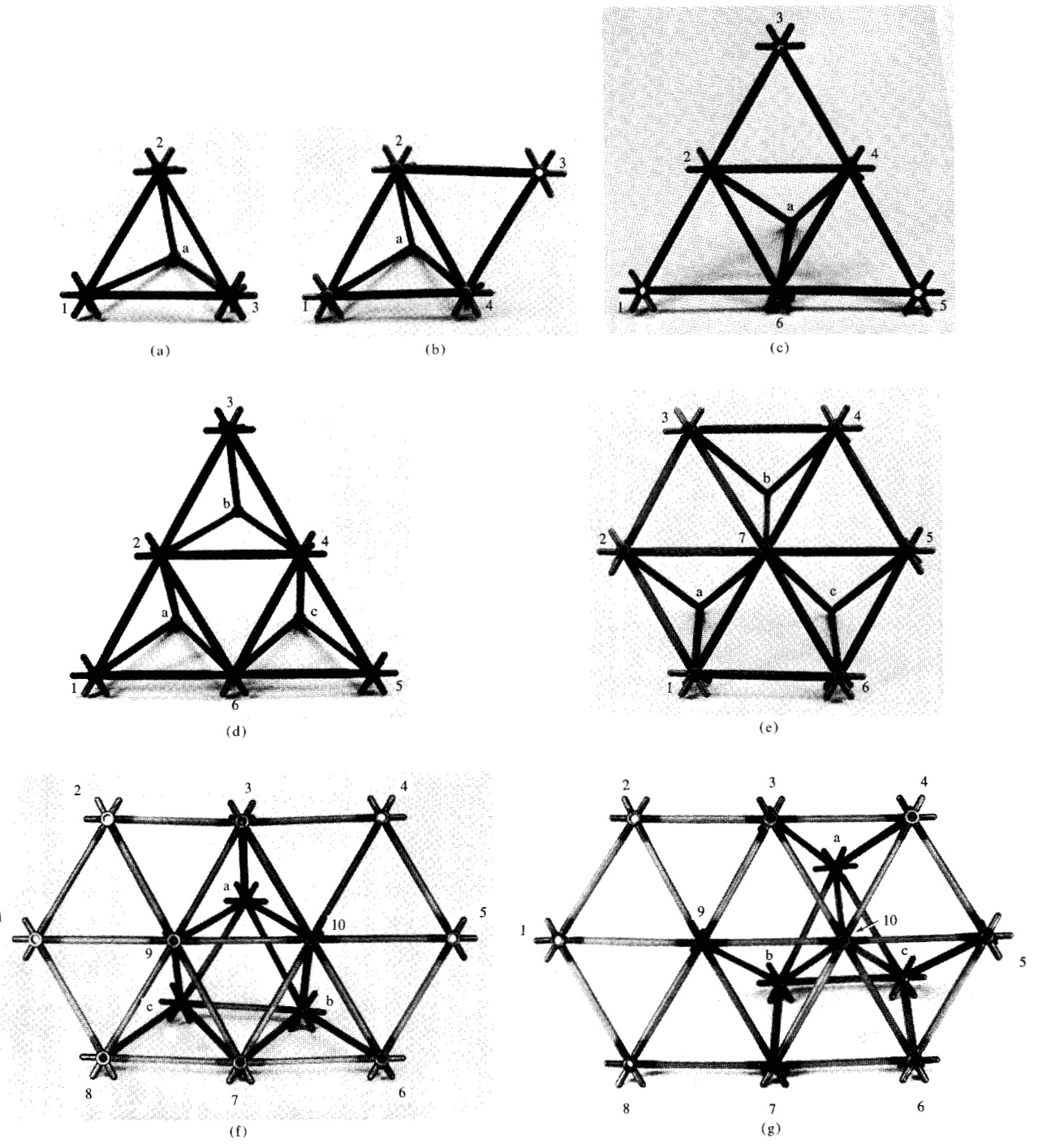


Figure A1 Cluster structures: (a) $Be_4(3,1)$, (b) $Be_5(4,1)$, (c) $Be_7(6,1)$, (d) $Be_9(6,3)$, (e) $Be_{10}(7,3)$, (f) $Be_{13}(10,3)A$, and (g) $Be_{13}(10,3)B$.

Appendix B: Basis sets

The basis sets used in this work are tabulated in Tables A1-A5, and are described below.

1. *Minimum Basis Set 1*. Here 1s, 2s, and 2p functions on Be were used and a single 1s function was centered on

hydrogen. Each function was a three-Gaussian expansion [63] of a Slater function. The Slater function exponents were those of Clementi and Raimondi [64]: $\zeta(1s) = 3.685$ and $\zeta(2s) = 0.956$. The 2p exponent, $\zeta(2p) = 0.890$, was optimized [65] for the ${}^{3}P(1s^{2}2s2p)$ state of Be. Finally, for the hydrogen atom $\zeta(1s) =$

Table A1 Be Minimum Basis Set I. Each function is a three-Gaussian fit to a single Slater exponent.

Type	Gaussian exponent	Contraction coefficient	Slater parameters
	30.249896	0.154329	
s	5.510056	0.535328	$\zeta(1s) = 3.685$
	1.491243	0.444635	3. ,
	2.359399	-0.059945	
s	0.143270	0.596039	$\zeta(2s) = 0.959$
	0.055003	0.458179	5. ,
	0.728128	0.162395	
р	0.186871	0.566171	$\zeta(2p) = 0.89$
•	0.063446	0.422307	J. 1

Table A2 Be Minimum Basis Set II.

	Set IIa	p Coefficient	
Exponent	s Coefficient		
0.994203	-0.099672	0.155916	
0.231031	0.399513	0.607684	
0.0751386	0.700115	0.391957	
	Set IIb		
Type	Exponent	Coefficient	
	2.581580	-0.059945	
S	0.156762	0.596039	
	0.060183	0.458179	
	0.919238	0.162395	
p	0.235919	0.566171	
_	0.080098	0.422307	

Table A3 Be Minimum Basis Set III. The 1s functions are the same as for Minimum Basis Set I. The 2s and 2p functions are fit to Slater exponents optimized for $Be_{10}(10,0)$.

Type	Gaussian exponent	Contraction coefficient	Slater parameters
	2.633470	-0.059945	
s	0.159913	0.596039	$\zeta(2s) = 1.01$
	0.061393	0.458179	3 ()
	0.882836	0.162395	
р	0.226577	0.566171	$\zeta(2p) = 0.98$
•	0.076926	0.422307	

1.15 was adopted. The atomic SCF energies obtained with this basis were Be, -391.632 eV [66], and H, -13.168 eV. The minimum basis set Slater SCF energy [64] is -396.117 eV.

- 2. Minimum Basis Set IIa. The hydrogen basis set remained the same, as did the Be 1s function. The Be 2s and 2p Slater exponents were constrained to be equal and were optimized for the Be₁₃(10,3)A cluster, $\zeta = 1.00$ [see Appendix A, Fig. A1(f)]. An additional constraint imposed, as a computational device, was that the 2s and 2p Slater functions be fit to the same three Gaussian functions.
- 3. Minimum Basis Set IIb. This basis set is the same as Minimum Basis Set IIa, except that the 2s and 2p functions were fit separately to the best three-Gaussian fit. The choice between using IIa or IIb depended upon which system of programs was being used; for some, the constrained fit offered a significant computational advantage.
- 4. Minimum Basis Set III. The Be 2s and 2p functions were optimized separately for the $Be_{10}(10,0)$ cluster.
- 5. Double Zeta Set I. This basis is a contracted Gaussian set of Be(9s2p/4s2p) and H(4s1p/2s1p). The Be s functions are from van Duijnevelt [67], and are contracted (6,1,1,1) to yield an SCF energy of -396.490 eV (-14.5704 hartrees); the Hartree-Fock energy [68] is -396.560 eV (-14.5730 hartrees). The two Be p functions were taken from a previous study [69] on BeF₂. For the hydrogen atom, van Duijneveldt's [67] s set was contracted (3,1) and a scale factor of 1.2 was applied. This basis yields an energy of -13.543 eV (-0.4977 hartree). A set of p functions with α = 1.0 was added [37].
- 6. *Double Zeta Set II*. The H basis set and the Be s functions are unchanged, but a set of four p functions replaced the previous set of p functions. The functions were optimized for Be(³P) [70].

References and notes

- A. Clark, The Chemisorptive Bond, Academic Press, Inc., New York, 1974.
- H. F. Schaefer, The Electronic Structure of Atoms and Molecules: A Survey of Rigorous Quantum Mechanical Results, Addison-Wesley Publishing Co., Inc., Reading, MA, 1972.
- R. C. Baetzold, J. Chem. Phys. 55, 4363 (1971); J. Solid State Chem. 6, 352 (1973); J. Catalysis 29, 129 (1973).
- J. C. Robertson and C. W. Wilmsen, J. Vac. Sci. Technol. 8, 53 (1971); 9, 901 (1972).
- D. J. M. Fassaert, H. Verbeek, and A. van der Avoird, Surface Sci. 29, 501 (1972); H. Deuss and A. van der Avoird, Phys. Rev. B 8, 2441 (1973).
- G. Blyholder, J. Chem. Soc. Chem. Commun. 625 (1973); Surface Sci. 42, 249 (1974).
- L. W. Anders, R. S. Hansen, and L. S. Bartell, J. Chem. Phys. 59, 5277 (1973); 62, 1641 (1975).
- K. H. Johnson and R. P. Messmer, J. Vac. Sci. Technol. 11, 236 (1974).
- A. B. Anderson and R. Hoffmann, J. Chem. Phys. 61, 4545 (1974).
- R. C. Baetzold and R. E. Mack, J. Chem. Phys. 62, 1513 (1975); Inorg. Chem. 14, 686 (1975).
- I. P. Batra and O. Robaux, Surface Sci. 49, 653 (1975); J. Vac. Sci. Technol. 12, 242 (1975).

- 12. S. J. Niemczyk, J. Vac. Sci. Technol. 12, 246 (1975).
- 13. A. L. Companion, Chem. Phys. 14, 1 (1976).
- J. G. Fripiat, K. T. Chow, M. Boudart, J. B. Diamond, and K. H. Johnson, J. Mol. Catal. 1, 59 (1975).
- 15. A. B. Anderson, Chem. Phys. Lett. 35, 498 (1975).
- 16. A. L. Companion, Chem. Phys. 14, 7 (1976).
- H. Stoll and H. Preuss, *Phys. Status Solidi* (B) 53, 519 (1972).
- W. C. Ermler, Ph.D. Thesis, Ohio State University, Columbus, OH, 1972.
- A. B. Kunz, D. J. Mickish, and P. W. Deutsch, Solid State Commun. 13, 35 (1973).
- C. F. Melius, J. W. Moskowitz, A. P. Mortola, M. B. Baillie, and M. A. Ratner, Surface Sci. 59, 279 (1976).
- C. W. Bauschlicher, D. H. Liskow, C. F. Bender, and H. F. Schaefer, J. Chem. Phys. 62, 4815 (1975).
- W. A. Goddard, paper presented at the Summer Research Conference on Theoretical Chemistry, Boulder, CO, June, 1975
- E. G. Derouane, J. G. Fripiat, and J. M. Andre, Chem. Phys. Lett. 35, 525 (1975).
- C. W. Bauschlicher, C. F. Bender, H. F. Schaefer, and P. S. Bagus, *Chem. Phys.* 15, 227 (1976).
- 25. C. S. Bowring and V. T. Wynn, *Phys. Lett.* 33, 401 (1970).
- P. S. Bagus, C. M. Moser, P. Goethals, and G. Verhaegen, J. Chem. Phys. 58, 1886 (1973).
- 27. R. Colin and D. DeGraf, Can. J. Phys. 53, 2142 (1975).
- 28. J. R. Schrieffer, J. Vac. Sci. Technol. 9, 561 (1971).
- 29. C. L. Pekeris, Phys. Rev. 112, 1649 (1958); 126, 1470 (1962).
- R. C. Jerner and C. B. Magee, Oxidation of Metals 2, 1 (1970).
- (a) R. O. Adams, The Structure and Chemistry of Solid Surfaces, G. A. Somorjai, ed., John Wiley & Sons, Inc., New York, 1969, p. 70;
 (b) J. J. Hurd and R. O. Adams, J. Vac. Sci. Technol. 5, 183
- J. M. Baker and J. M. Blakely, J. Vac. Sci. Technol. 8, 56 (1971); R. S. Zimmer and W. D. Robertson, Surface Sci. 43, 61 (1974).
- D. M. Zehner, N. Barbulesco, and L. H. Jenkins, Surface Sci. 34, 385 (1973); R. G. Musket and R. J. Fortner, Phys. Rev. Lett. 26, 80 (1971); M. Suleman and E. B. Pattinson, J. Phys. F. (Met. Phys.) 1, L24 (1971); 3, 497 (1973); R. G. Musket, Surface Sci. 44, 629 (1974).
- 34. J. Donohue, *The Structure of the Elements*, Wiley Interscience Publishers, New York, 1974.
- For the use of four indices to define directions in a hexagonal structure, see C. Kittel, *Introduction to Solid State Physics*, John Wiley & Sons, Inc., New York, 1956, p. 35.
- 36. The basis set parameters are described in [2], Section 1D, and references therein.
- B. Roos and P. Siegbahn, *Theoret. Chim. Acta* 17, 199 (1970).
- 38. R. K. Nesbet, Proc. Roy. Soc. A 230, 312 (1955).
- See, for example, F. A. Cotton, Chemical Applications of Group Theory, Wiley Interscience Publishers, New York, 1971.
- 40. E. R. Davidson, Rev. Mod. Phys. 44, 451 (1972).
- 41. C. C. J. Roothaan, Rev. Mod. Phys. 23, 69 (1951).
- P. S. Bagus and U. I. Wahlgren, Computers and Chemistry 1, 95 (1976).
- 43. A. D. McLean and B. Liu, J. Chem. Phys. 58, 1066 (1973).
- B. Cartling, B. Roos, and U. I. Wahlgren, Chem. Phys. Lett. 21, 380 (1973).
- 45. J. C. Slater, *Phys. Rev.* **35**, 509 (1930).
- 46. R. S. Mulliken, J. Chem. Phys. 23, 1833 (1955).
- R. S. Mulliken, J. de Chimie Physique 46, 497 (1949); P. S. Bagus, Phys. Rev. A 139, 619 (1965); D. A. Shirley, Chem. Phys. Lett. 16, 220 (1972).
- JANAF Thermochemical Tables, PB168-370-2, distributed by Clearinghouse for Federal Scientific and Technical Information (1965).

Table A4 Be Double Zeta Basis Sets I and II. Both sets have the same s basis and differ in the p basis.

Туре	Exponent	Coefficient	
s	2732.328145 410.319811 93.672648 26.587957 8.629560 3.056264	$ \begin{pmatrix} 0.000745 \\ 0.005724 \\ 0.028888 \\ 0.107092 \\ 0.280109 \\ 0.446089 \end{pmatrix} $	
	1.132424	1.000000	
	0.181732	1.000000	
	0.059170	1.000000	
Basis I: p	0.509	1.000000	
	0.118	1.000000	
Basis II: p	$ \left\{ \begin{array}{l} 3.202 \\ 0.6923 \\ 0.2016 \end{array} \right. $	$ \begin{pmatrix} 0.052912 \\ 0.267659 \\ 0.792085 \end{pmatrix}$	
	0.06331	1.000000	

Table A5 Hydrogen basis sets.

Set	Type	Exponent	Coefficient
Minimum	S	$ \left\{ \begin{array}{l} 2.94608 \\ 0.536632 \\ 0.145234 \end{array}\right\} $	0.154329 0.535328 0.444635
Double Zeta	s	\begin{cases} 18.73925 \\ 2.825994 \\ 0.640179 \end{cases}	0.019678 0.137952 0.478313
		0.175612	1.0
	p	1.0	1.0

- 49. The ε cannot be used directly as Koopmans' theorem IPs for open-shell systems. The closed-shell ε are IPs to an average of singlet and triplet states of Be₂₂-H⁺. See P. A. Cox, Mol. Phys. 30, 389 (1975).
- C. C. J. Roothaan, Rev. Mod. Phys. 32, 179 (1960); C. C. J. Roothaan and P. S. Bagus, Methods in Computational Physics 2, 47 (1963).
- 51. R. Lavery and I. H. Hillier, Chem. Phys. 16, 281 (1976).
- J. A. Pople and D. L. Beveridge, Approximate Molecular Orbital Theory, McGraw-Hill Book Co., Inc., New York, 1970
- N. D. Lang and A. R. Williams, Phys. Rev. Lett. 34, 531 (1975).
- S. W. Marisa Wang and W. H. Weinberg, Surface Sci., in press.
- 55. J. R. Smith, Phys. Rev. 181, 522 (1969).
- H. Froitzheim, H. Ibach, and S. Lehwald, *Phys. Rev. Lett.* 36, 1549 (1976).

- G. Herzberg, Molecular Spectra in Molecular Structure 1. Spectra of Diatomic Molecules, Van Nostrand, New York, 1950.
- 58. D. P. Smith, *Hydrogen in Metals*, University of Chicago Press, Chicago, 1948.
- 59. D. L. Mills, Surface Sci. 48, 59 (1975).
- 60. K. Hermann and P. S. Bagus, Phys. Rev. B, in press.
- V. Bonifacic and S. Huzinaga, J. Chem. Phys. 60, 2779 (1974); 62, 1507, 1509 (1975).
- C. F. Melius, B. D. Olafson, and W. A. Goddard III, Chem. Phys. Lett. 28, 457 (1974).
- W. J. Hehre, R. F. Steward, and J. A. Pople, Symp. Faraday Soc. 2, 15 (1968).
- E. Clementi and D. L. Raimondi, J. Chem. Phys. 38, 2686 (1963).
- 65. These energies are sometimes given in hartrees. One hartree is equal to twice the value of the Rydberg constant R_{∞} , or 27.212 eV. The values of the atomic SCF energies for Be and H in these units are -14.3919 and -0.4839 hartrees, respectively; the Slater SCF energy is -14.5567 hartrees.
- 66. T. Dunning, unpublished results.
- 67. F. B. van Duijneveldt, *Research Report RJ 945*, IBM Research Laboratory, San Jose, CA, 1971.

- P. S. Bagus, T. L. Gilbert, and C. C. J. Roothaan, J. Chem. Phys. 56, 5195 (1972).
- S. Rothenberg and H. F. Schaefer, J. Amer. Chem. Soc. 95, 2095 (1973).
- D. R. Yarkony and H. F. Schaefer, J. Chem. Phys. 61, 4921 (1974).

Received November 14, 1977

C. W. Bauschlicher, Jr., is currently located at the Institute for Computer Applications in Science and Engineering, NASA Langley AFB, Hampton, Virginia 23665; P. S. Bagus is located at the IBM Research Division Laboratory, 5600 Cottle Road, San Jose, California 95193; and H. F. Schaefer is a member of the Department of Chemistry and Materials and Molecular Division at the Lawrence Berkeley Laboratory, University of California, Berkeley, California 94720.